Random matrix approaches to open quantum systems

Henning Schomerus
Department of Physics, Lancaster University, Lancaster, LA1 4YB, UK

Contents

1
Introduction

1.1 Welcome

Open quantum systems come in two variants. The first variant (on which we will focus more) are scattering systems in which the dynamics allow particles to enter and leave (Newton, 2002; Messiah, 2014). One then normally defines a scattering region, outside of which particles move free of any external forces or interactions. This situation is realised (at least to some level of approximation) in many decay or radiation processes (Weidenmüller and Mitchell, 2009), but is also useful to describe phase-coherent transport in mesoscopic devices (Datta, 1997; Beenakker, 1997; Blanter and Büttiker, 2000; Nazarov and Blanter, 2009) or photonic structures (Cao and Wiersig, 2015). The second variant (which we will encounter only briefly) are interacting systems in which the studied dynamical degrees of freedom are influenced by other degrees of freedom in the environment (Breuer and Petruccione, 2002). This situation spans from the quantum-statistical foundations of thermodynamics (Gemmer *et al.*, 2010) to the description of decoherence (Weiss, 2008), with ample applications to quantum optics (Carmichael, 2009), quantum-critical phenomena (Sachdev, 1999) and quantum information processing (Nielsen and Chuang, 2010).

While these two scenarios of openness are in many ways quite distinct, they have some important features in common—in particular, in both scenarios we are led to restrict our attention to a subsystem, while the processes that are involved often are very complex (meaning that we have no realistic handles to describe them in detail), be it due to underlying classical chaos, disorder, or uncontrolled interactions. Taken together, these features lay the foundations for a statistical description where individual systems are replaced by an appropriate ensemble. These ensembles are typically formulated in terms of effective models, e.g., for the Hamiltonian, the scattering matrix, or the density matrix, in which only the fundamental symmetries and the most essential time and energy scales are retained. Quantitative predictions then follow from explicit calculations and often turn out to be universal, i.e., applicable to generic representatives of the ensemble.

Over the past decades, a great body of theoretical and mathematical work has been devoted to these random-matrix descriptions (Beenakker, 1997; Guhr *et al.*, 1998; Mehta, 2004; Stöckmann, 2006; Haake, 2010; Forrester, 2010; Akemann *et al.*, 2011; Pastur and Shcherbina, 2011; Beenakker, 2015). In these notes we review the physical origins and mathematical structures of the underlying models, and collect key predictions which give insight into the typical system behaviour. In particular, we aim to give an idea how the different features are interlinked. This includes a detour to interacting systems, which we motivate by the overarching question of ergodicity.

With this selection of topics, we hope to provide a useful bridge to the many excellent advanced sources, including the monographs and reviews mentioned above, which contain detailed expositions of the random-matrix calculations and further applications not covered here. In the remainder of this introduction, we provide some basic background.

1.2 Primer

These lectures were delivered to a mixed audience of mathematicians and physicists. To establish some common language, let us first review some basic notions of quantum mechanics (Peres, 2002). This also gives us the opportunity to pinpoint the fundamental origins of the mathematical concepts and physical phenomena that we will encounter throughout these notes—and further explain what these notes are really about.

Let us recall, then, that quantum mechanics describes the physical states of a system in terms of vectors $|\psi\rangle$, $|\phi\rangle, \ldots$ in a complex Hilbert space $\mathcal{H}$. The superposition principle means that the vectors can be freely combined to yield new physical states $\alpha|\psi\rangle + \beta|\phi\rangle$, $\alpha, \beta \in \mathbb{C}$. All vectors $\alpha|\psi\rangle$ that differ only by a multiplicative factor $\alpha \neq 0$ describe the same physical state, which is often exploited to impose the convenient normalization $\langle\psi|\psi\rangle = 1$. Following physics convention, we here use (what we term) the scalar product with $\langle\phi|(\alpha\psi + \beta\chi)\rangle = \alpha\langle\phi|\psi\rangle + \beta\langle\phi|\chi\rangle$, $\langle\psi|\phi\rangle = \langle\phi|\psi\rangle^*$, $\langle\psi|\psi\rangle > 0$ unless $|\psi\rangle = 0$, where * denotes complex conjugation. Two states with $\langle\phi|\psi\rangle = 0$ are called orthogonal, and a discrete basis with $\langle n|m\rangle = \delta_{nm}$ is called orthonormal. For a continuous basis, this is replaced by $\langle x|x'\rangle = \delta(x - x')$ with Dirac's delta function. In a given basis, states can be expanded as $|\psi\rangle = \sum_n \psi_n|n\rangle$ where $\psi_n = \langle n|\psi\rangle$, with the sum replaced by an integral when the basis is continuous.

Observables are represented by hermitian linear operators $\hat{A}$, with $\hat{A}|\psi\rangle \equiv |\hat{A}\psi\rangle \in \mathcal{H}$ such that $\langle\phi|\hat{A}\psi\rangle = \langle\hat{A}\phi|\psi\rangle$. According to the measurement axiom, these operators predict physical observations via the expectation values $\mathcal{E}_\psi(A) = \langle\psi|\hat{A}\psi\rangle/\langle\psi|\psi\rangle$, which in reality are obtained by averaging the outcomes of experiments on systems in the same quantum state. The associated uncertainty (variance) is obtained from $\Delta A = [\mathcal{E}_\psi(A^2) - \mathcal{E}_\psi^2(A)]^{1/2}$, which in general is finite. Denoting by $E_a = \sum_n |\psi_{a,n}\rangle\langle\psi_{a,n}|$ the projector onto states that guarantee an outcome a with vanishing uncertainty $\Delta A = 0$, one finds that these are eigenstates with $\hat{A}|\psi_{a,n}\rangle = a|\psi_{a,n}\rangle$. In a general state, the probability of these outcomes $|\psi\rangle$ are then $P(a) = \langle\psi|E_a|\psi\rangle/\langle\psi|\psi\rangle$; no outcomes other than the associated eigenvalues are allowed. Beyond this probabilistic description, outcomes of individual experiments are unpredictable. Finally, the measurement axiom stipulates that right after the measurement with an outcome a, the quantum system acquires the state $E_a|\psi\rangle$.

Adopting the conventional Schrödinger picture, the time dependence of the quantum state arises from the Schrödinger equation

$$i\hbar\frac{d}{dt}|\psi(t)\rangle = \hat{H}(t)|\psi(t)\rangle. \tag{1.1}$$

Here $\hat{H}$ is the Hamiltonian, a hermitian operator which represents energy, while $\hbar = h/2\pi$ is the reduced Planck's constant. The general solution can be written as

$|\psi(t)\rangle = \hat{U}(t,t')|\psi(t')\rangle$, where $\hat{U}(t,t')$ is a unitary operator ($\hat{U}$ is unitary if always $\langle\hat{U}\phi|\hat{U}\psi\rangle = \langle\phi|\psi\rangle$). If $\hat{H}$ is independent of time, we can separate variables as $|\psi(t)\rangle = \exp(-iEt/\hbar)|\phi\rangle$ and arrive at the stationary Schrödinger equation $E|\phi\rangle = \hat{H}|\phi\rangle$. In this case, $\hat{U}(t,t') = \exp(-i\hat{H}(t-t')/\hbar)$.

In order to describe the incoherent mixture of normalised quantum states $|\psi_n\rangle$ one introduces the density matrix (statistical operator) $\hat{\rho} = \sum_n p_n|\psi_n\rangle\langle\psi_n|$ with positive weights p_n summing to $\sum p_n = 1$, so that $\mathrm{tr}\,\hat{\rho} = 1$. The expectation values $\mathcal{E}_\rho(A) = \mathrm{tr}\,(\hat{A}\hat{\rho}) = \sum_n p_n \mathcal{E}_{\psi_n}(A)$ are a combination of the quantum-mechanical average in each quantum state and the classical average over the weights p_n. The density operator is hermitian and positive semidefinite, and for a pure state (with only one finite $p_n = 1$) becomes a projector, $\hat{\rho}^2 = \hat{\rho}$. To capture the departure from this situation one can consider the purity $\mathcal{P} = \mathrm{tr}\,\hat{\rho}^2$, which equals unity only for a pure state, as well as the von Neumann entropy $\mathcal{S} = -\mathrm{tr}\,\hat{\rho}\ln\hat{\rho}$, which vanishes for a pure state.

1.3 Open systems

The superposition principle mentioned above is the origin of wave-like interference effects, the complexity of which we will aim to capture in a statistical description. To provide the states with some structure, we can often think of the state space being divided into sectors (which we here call regions), $\mathcal{H} = \mathcal{H}_1 \oplus \mathcal{H}_2$. We then can start to talk about local and non-local processes, within or between the regions, and introduce basic notions such as the exchange of particles or energy. An additional layer of complexity is added when we can view the system as being composed of separate degrees of freedom (which we here call parts). The Hilbert space then takes the form of a tensor product $\mathcal{H} = \mathcal{H}_1 \otimes \mathcal{H}_2$, with proper symmetrization or antisymmetrization if the parts are, in a physical sense, indistinguishable (e.g., when they describe identical bosonic or fermionic particles). Separable states are of the form $|\phi\rangle \otimes |\chi\rangle$, while superpositions of such states lead to quantum correlations (entanglement) that deeply enrich the behaviour of interacting systems. Based on these elements of structure, let us now agree, within the confines of these notes, on two notions of open quantum systems. These are systems in which we can naturally focus on some region or part $\mathcal{H}_1$, which is either locally confined (as in $\mathcal{H} = \mathcal{H}_1 \oplus \mathcal{H}_2$) or constrained to some of the degrees of freedoms (as in $\mathcal{H} = \mathcal{H}_1 \otimes \mathcal{H}_2$). We are then naturally led down two roads: Scattering-like scenarios, which describe the exchange of particles between a confined region and its surrounding environment, and scenarios dominated by the interactions, which often concern the exchange of energy and creation of entanglement. In order for this division to make some sense, the environment must be sufficiently structureless—either because the dynamics are simple and predictable (typically, the point of view taken in the case of scattering), or because they are so complex that they can be described in a simple statistical picture (typically, the point of view taken in the case of interactions). Physically, this requires that the rest of the system is large, and of a nature where incoming and outgoing particles are only simply correlated, and so is the energy flowing in or out of the system.

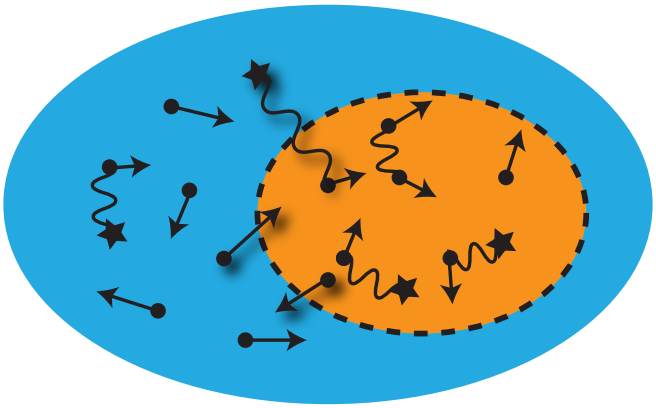

Fig. 1.1 Quantum systems couple to their environment by the exchange of particles and energy, and thereby by processes connected to the kinetic freedom of motion and the interactions of the various components.

1.4 Preview

With these concepts at hand, we can now define our mission—to provide a statistical description of open quantum systems in terms of random matrices. This succeeds in situations where we can apply statistical considerations also to the complex dynamics in the region or part of interest, with constraints only arising from fundamental symmetries. We describe both settings in their purest incarnation.

(i) Our main focus is the elastic scattering of a non-interacting particle, which can undergo complex dynamics in the region of interest but enters and leaves in predictable ways. This is quantified in terms of the amplitudes of the incoming and outgoing waves, which are linearly related by a unitary scattering matrix S. As this pure setting is stationary, we can work in the energy domain, while time scales follow when we consider variations in energy. This setting also covers decay processes, where we initially confine the particle within the region of interest—effectively, this is described by a non-hermitian Hamiltonian, with eigenvalues that coincide with the poles of the scattering matrix.

(ii) In a small detour at the end of these notes, we consider purely interacting systems, with localized degrees of freedom that cannot move but evolve under the influence of their mutual environment. We quantify this in terms of a reduced density matrix, a hermitian, positive semidefinite matrix which represents the quantum state when one ignores the other degrees of freedom. We again assume complex internal dynamics, and consider entropies that quantify entanglement.

As indicated, we will encounter, amongst others, random hermitian Hamiltonians, unitary scattering matrices, positive semidefinite density and time-delay matrices, and non-hermitian effective Hamiltonians. These are all naturally linked to canonical random-matrix ensembles (not surprisingly, as many of these ensembles were developed with such applications in mind), which we review in Chapter 2. In Chapter 3 we formulate effective scattering models that link these ensembles to physical effects.

Chapter 4 provides an overview of key results concerning the decay, dynamics and transport, where we focus on systems with fully random internal dynamics. Chapter 5 describes how localizing effects in low dimensions let systems depart from this ergodic behaviour, first for non-interacting systems and then in the context of interacting systems. Chapter 6 gives a brief outlook, while the Appendix collects some simple derivations of relevant eigenvalue densities.

2
Foundations of random-matrix theory

In this chapter we review a range of classical random-matrix ensembles against the backdrop of closed-system behaviour, which informs the subsequent applications to open systems.

2.1 Random Hamiltonians and Gaussian hermitian ensembles

Random-matrix descriptions in quantum mechanics naturally start out with considerations of closed systems. In this setting, the main object of interest is the Hamiltonian $\hat{H}$, whose eigenvalues give the energy levels. The energy spectrum can be characterised very neatly if one manages to identify a number of conserved quantities that commute with the Hamiltonian and amongst each other; considering joint eigenstates of these quantities helps to bring some order to the spectrum. In sufficiently complex systems, however, effects such as chaotic or diffractive scattering and interactions eliminate all conserved quantities, and the energy spectrum lacks any apparent regularities. It is natural to compare the resulting features with the case where the Hamiltonian can be considered as random. This was first proposed in the 1950's by Wigner (1956), who sought ways to analyse resonances in heavy nuclei. The idea is to focus on a suitable energy range, where the local spectral properties can then be studied by replacing the full Hamiltonian with a randomly chosen $M \times M$-dimensional hermitian matrix (the limit $M \to \infty$ can be imposed later on).

The quality of this descriptions depends on the identification of a suitable random-matrix ensemble. To achieve this task we are allowed to incorporate any general feature of the system. These are, in particular, fundamental symmetries, rough geometric constraints such as dimensionality, as well as natural time and energy scales.

The consideration of fundamental symmetries leads to ten symmetry classes (Zirnbauer, 1996; Zirnbauer, 2011; Beenakker, 2015). These comprise the three Wigner-Dyson classes based on time-reversal symmetry (Dyson, 1962*a*; Porter, 1965; Mehta, 2004; Guhr *et al.*, 1998; Haake, 2010), three corresponding classes with chiral symmetry (Verbaarschot, 1994; Verbaarschot and Wettig, 2000), and four classes based on a charge-conjugation symmetry (Altland and Zirnbauer, 1997). These classes are developed in the present section, and listed in Table 2.1. We also describe the corresponding hermitian matrix ensembles for the simplest situation, geometrically featureless systems in which the only relevant energy scale is the mean level spacing Δ. This reasonably applies when all system-specific information becomes indiscernible

after a short time $T_{\rm erg}$, which in particularly is much shorter than the Heisenberg time $T_H = 2\pi\hbar/\Delta$ (the minimal observation time at which individual energy levels can be resolved). Examples where this is realised are sufficiently featureless disordered (Efetov, 1996) or classically chaotic systems (Stöckmann, 2006; Haake, 2010). The short-ranged level statistics then becomes universal, and can be captured by ensembles with Gaussian statistics of the matrix elements (Mehta, 2004; Guhr *et al.*, 1998; Haake, 2010; Forrester, 2010).

2.1.1 Time-reversal symmetry and the Wigner-Dyson ensembles

We start by considering the role of time reversal (Dyson, 1962*a*; Haake, 2010), instituted by an anti-unitary operator $\mathcal{T}$ fulfilling $\langle\mathcal{T}\phi|\mathcal{T}\psi\rangle = \langle\psi|\phi\rangle = \langle\phi|\psi\rangle^*$, which consequently may square to $\mathcal{T}^2 = 1$ or $\mathcal{T}^2 = -1$.

If the Hamiltonian obeys a time-reversal symmetry $\mathcal{T}H\mathcal{T}^{-1} = H$ with $\mathcal{T}^2 = 1$, we can adopt an invariant basis $|n\rangle$ in which $\langle\mathcal{T}n|\psi\rangle = \langle n|\psi\rangle$ for any $|\psi\rangle$. This implies $\langle n|\mathcal{T}\psi\rangle = \langle n|\psi\rangle^*$, so that the time-reversal operation $\mathcal{T} = K$ amounts to the complex conjugation of the expansion coefficients $\psi_n = \langle n|\psi\rangle$ of any state. In this basis the matrix elements $H_{lm} = \langle l|\hat{H}|m\rangle = \langle\mathcal{T}l|\hat{H}\mathcal{T}|m\rangle = H^*_{lm}$ are real, while hermiticity implies that the matrix is symmetric, $H_{ml} = H_{lm}$. This is known as the *orthogonal symmetry class* (OE), to which we associate the symmetry index $\beta = 1$.

In absence of any time-reversal symmetry, matrix elements of the Hamiltonian are in general complex, with $H_{lm} = H^*_{ml}$ because of hermiticity, which defines the *unitary symmetry class* (UE) with symmetry index $\beta = 2$.

If we have a time-reversal symmetry $\mathcal{T}H\mathcal{T}^{-1} = H$ with $\mathcal{T}^2 = -1$ (*symplectic symmetry class* SE with symmetry index $\beta = 4$), we can adopt a basis arranged in pairs $|n\rangle = \mathcal{T}|\bar{n}\rangle$, so that the Hilbert space dimension $2M$ must be even. In this basis,

Table 2.1 Fundamental symmetries of hermitian random-matrix ensembles

symmetries	constraints	realization ($H^*_{mn} = H_{nm}$)
no symmetries	none besides $H = H^\dagger$	$H_{nm} \in \mathbb{C}$
$\mathcal{T} = K$	$H^* = H$	$H_{nm} \in \mathbb{R}$
$\mathcal{T} = \Omega K$	$H^* = \Omega H \Omega^{-1}$	$H_{nm} \in \mathbb{H}$
$\mathcal{C} = K$	$H^* = -H$	$H_{nm} \in i\mathbb{R}$
$\mathcal{C} = K$, $\mathcal{T} = \Omega K$	$H^* = -H = \Omega H \Omega^{-1}$	$H_{nm} = -\sigma_y H_{nm} \sigma_y \in \mathbb{H}$
$\mathcal{C} = \Omega K$	$H^* = -\Omega H \Omega^{-1}$	$H_{nm} \in i\mathbb{H}$
$\mathcal{C} = \Omega K$, $\mathcal{T} = K$	$H^* = H = -\Omega H \Omega^{-1}$	$H_{nm} = -\sigma_y H_{nm} \sigma_y \in i\mathbb{H}$
$\mathcal{X} = \tau_z \equiv \mathrm{diag}\,(1_{M_1}, -1_{M_2})$	$H = -\tau_z H \tau_z$	$H = \begin{pmatrix} 0 & A \\ A^\dagger & 0 \end{pmatrix}$, $A_{nm} \in \mathbb{C}$
$\mathcal{X} = \tau_z$, $\mathcal{C} = K$ $(\mathcal{T} = \mathcal{X}\mathcal{C})$	$H = -\tau_z H \tau_z = -H^*$	$H = \begin{pmatrix} 0 & A \\ A^\dagger & 0 \end{pmatrix}$, $A_{nm} \in i\mathbb{R}$
$\mathcal{X} = \tau_z$, $\mathcal{C} = \Omega K$ $(\mathcal{T} = \mathcal{X}\mathcal{C})$	$H = -\tau_z H \tau_z = -\Omega H^* \Omega^{-1}$	$H = \begin{pmatrix} 0 & A \\ A^\dagger & 0 \end{pmatrix}$, $A_{nm} \in i\mathbb{H}$

$T = \Omega K$ where $\Omega = i\sigma_y \otimes 1_M$, while the blocks $\begin{pmatrix} H_{lm} & H_{l\bar{m}} \\ H_{\bar{l}m} & H_{\bar{l}\bar{m}} \end{pmatrix} = a_{lm}1 + ib_{lm}\sigma_x + ic_{lm}\sigma_y + id_{lm}\sigma_z \in \mathbb{H}$ can be reinterpreted as quaternions, with real coefficients $a_{lm}, b_{lm}, c_{lm}, d_{lm}$ and Pauli matrices σ_r. Hermiticity requires that $a_{lm} = a_{ml}$ forms a symmetric matrix while $b_{lm} = -b_{ml}$, $c_{lm} = -c_{ml}$, $d_{lm} = -d_{ml}$ are antisymmetric. Expressed as an $M \times M$-dimensional matrix of quaternions, $H = \overline{H}$ is then seen to be quaternion self-conjugate, where by definition $(\overline{H})_{lm} = \overline{H_{ml}} = a_{ml}1 - ib_{ml}\sigma_x - ic_{ml}\sigma_y - id_{ml}\sigma_z$. For such a matrix, all energy levels appear in degenerate pairs, a phenomenon known as Kramers degeneracy; in all following considerations we count each pair as a single level. In keeping with this, the quaternion trace is defined as $\operatorname{tr} H = \sum_n a_{nn}$ (so differs by a factor of two from the conventional trace), and the quaternion determinant is similarly modified to maintain the relation $\det \exp A = \exp \operatorname{tr} A$, which makes it equivalent to a Pfaffian (Dyson, 1970).

The symmetry index $\beta = 1, 2, 4$ mentioned above counts the real degrees of freedom in the matrix elements. The corresponding notions of orthogonal, unitary and symplectic symmetry classes refer to the transformations $H = U\,D\,U^\dagger$, $D = \operatorname{diag}(E_n)$ that diagonalise these Hamiltonians. For $\beta = 1$ the matrix U is orthogonal, $UU^T = 1$, and hence belongs to the group $\mathrm{O}(M)$; for $\beta = 2$ $U \in \mathrm{U}(M)$ is a unitary matrix with $UU^\dagger = 1$, and for $\beta = 4$ the matrix is unitary symplectic, $U \in \mathrm{Sp}(2M)$ with $U\overline{U} = 1$. This 'threefold way' can be further justified within representation theory (Dyson, 1962*c*).

Within these three Wigner-Dyson classes, the universal spectral features encountered in ergodic systems are captured by the Gaussian orthogonal, unitary, or symplectic ensemble (GOE, GUE, GSE), where the Hamiltonian obeys a probability density of the form $P(H) \propto \exp(-c_\beta \operatorname{tr} H^2)$ with $c_\beta = \beta\pi^2/4M\Delta^2$. The spectral statistics can then be determined from the joint probability distribution

$$P(\{E_n\}) \propto \prod_{n<m} |E_n - E_m|^\beta \prod_k \exp(-c_\beta E_k^2), \tag{2.1}$$

which follows by a change of variables from the Hamiltonian to its eigenvalues and eigenvectors. This result can be obtained by sophisticated methods in the language of differential geometry (Forrester, 2010), but in this specific incarnation also follows from elementary means and then acquires a simple geometric meaning. Given that $dH = dU\,D\,U^\dagger + U\,dD\,U^\dagger - U\,D\,U^\dagger U\,U^\dagger$, consider the squared line element

$$\sum_{lm} |dH_{lm}|^2 = \operatorname{tr}(dH\,dH) = \operatorname{tr}(dX\,D - D\,dX)^\dagger (dX\,D - D\,dX) + \sum_m (dE_m)^2, \tag{2.2}$$

where D contains M real parameters (the eigenvalues) while $dX = -iU^\dagger dU$ depends on $M(M-1)/2$ real, complex or quaternion parameters in the set of eigenvectors. The latter parameters can be associated with the rotations $R^{(nm)}$ in the nm plane of the diagonalised system, spanned by the eigenvectors with eigenvalues E_n and E_m. Each of these rotations then translates into a line element in the space of Hamiltonians of length $\propto |E_n - E_m|^\beta$, where the power arises from the fact that the rotation is parameterised by β real variables. (In particular, if we rotate the basis in a degenerate subspace the Hamiltonian does not change.) Hence $d\mu(H) \propto \left(\prod_{n<m} |E_n - E_m|^\beta\right) \left(\prod_k dE_k\right) d\mu(U)$,

where $\mu(U)$ is the Haar measure arising from the form dX in the corresponding group of transformations. This measure is uniquely defined by the requirement that it is invariant under $U \to V'UV$ for any fixed V, V' form the same group.

The main characteristics of (2.1) is a universal degree of level repulsion $P(s) \sim s^\beta$ for small level spacings $s = |E_n - E_m|$ in the bulk of the spectrum. This feature was first realised by Wigner, who put forward the famous surmise $P(s) \sim s^\beta \exp(-cs^2)$ with a suitable scale factor c (Porter, 1965). As it turned out, this surmise is exact only for $M = 2$, but provides a very accurate estimate for any M. The exact result can be established by the method of orthogonal polynomials (here based on Hermite polynomials), which provides the complete set of correlation functions (Mehta, 2004). When applied to a particular system, these correlations describe the short-ranged statistics in the bulk, i.e., over sufficiently small spectral ranges where the mean level spacing Δ is well defined (possibly, after some unfolding of the spectrum). In particular, the amount of level repulsion is considered as a prime indicator of whether a system displays the required ergodic dynamics, as further discussed in Chapter 5.

The mean level spacing itself is not universal; in real systems it varies systematically with energy, but for any comparison we wish to have it well defined in any given ensemble. In the Gaussian ensembles, this is guaranteed by the form of the eigenvalue density, which for large matrix dimensions $M \to \infty$ approaches the famous Wigner semicircle law (Wigner, 1958)

$$\rho(E) = \frac{1}{\Delta}\sqrt{1 - E^2/E_0^2} \quad \text{for } |E| < E_0 = 2M\Delta/\pi. \tag{2.3}$$

A derivation of this classical result is given in the Appendix. It reveals that $\Delta = 1/\rho(0)$ is the mean level spacing at $E = 0$, defining the middle of the bulk around which we then determine the universal spectral features. Universal level statistics are also encountered around the spectral edges $\pm E_0$, whose actual positions are again system specific.

2.1.2 Chiral symmetry

Additional positions within the spectrum deserve dedicated attention when further symmetries come into play. In particular, this is encoutered when the Hamiltonian is antisymmetric under a suitable unitary or antiunitary transformation, an effect which often occurs in single-particle descriptions of fermions. Energy levels then appear in pairs E_n, $E_{\tilde{n}} = -E_n$, with the possible exception of levels pinned to the spectral symmetry point $E = 0$.

If $\mathcal{X}H\mathcal{X} = -H$ with a unitary involution $\mathcal{X}$ (such that $\mathcal{X}^2 = 1$), we talk of a chiral symmetry (Verbaarschot, 1994; Verbaarschot and Wettig, 2000). For a finite system of dimension $M = M_1 + M_2$, we can choose $\mathcal{X} = \mathrm{diag}\,(1_{M_1}, -1_{M_2}) \equiv \tau_z$, so that the Hamiltonian takes a block form

$$H = \begin{pmatrix} 0 & A \\ A^\dagger & 0 \end{pmatrix} \tag{2.4}$$

where A is an $M_1 \times M_2$-dimensional rectangular matrix.

The chiral symmetry arises in elementary particle physics (Verbaarschot and Wettig, 2000; Akemann, 2017), but can also be realised as an effective symmetry in electronic (Brouwer *et al.*, 2002), superconducting (Fu and Kane, 2008) and photonic systems (Schomerus and Halpern, 2013; Lu *et al.*, 2014; Poli *et al.*, 2015). Given the structure (2.4), the symmetry generally applies to systems with two sublattices, termed A and B, when the couplings within each isolated sublattice vanish (Sutherland, 1986). The mentioned electronic and photonic implementations naturally extend this idea to suitably coupled subsystems.

An interesting aspect of these classes is the appearance of topological invariants, associated with the number of eigenenergies pinned to the symmetry point (Lieb, 1989; Verbaarschot, 1994; Brouwer *et al.*, 2002). For a Hamiltonian of the form (2.4) with some finite $\nu = M_2 - M_1$ (so that A is not square), there are at least $|\nu|$ such zero modes. If $\nu < 0$ the associated eigenstates are of the form $\psi = (\psi_A, 0)^T$ with $A^\dagger \psi_A = 0$, while for $\nu > 0$ we have $\psi = (0, \psi_B)^T$ with $A\psi_B = 0$. The remaining paired levels with finite energy can be determined from the positive definite matrix $A^\dagger A$ or $AA^\dagger$, whose eigenvalues are given by E_n^2.

In combination with considerations of time-reversal symmetry one can now define *chiral orthogonal, unitary or symplectic symmetry classes* (chOE, chUE, chSE) (Verbaarschot, 1994; Verbaarschot and Wettig, 2000; Akemann, 2017), which are again associated with a symmetry index $\beta = 1, 2, 4$. Taking A as a random matrix with real, complex, or quaternion entries and $P(A) \propto \exp(-c_\beta \operatorname{tr} A^\dagger A)$ then leads to the Gaussian chiral ensembles (chGOE, chGUE, and chGSE), for which the positive energy levels in each pair follow the joint distribution

$$P(\{E_n\}) \propto \prod_{n<m, E_{n,m}>0} |E_n^2 - E_m^2|^\beta \prod_{k, E_k>0} E_k^{(|\nu|+1)\beta-1} \exp(-c_\beta E_k^2). \tag{2.5}$$

The terms $E_n^2 - E_m^2 = (E_n - E_m)(E_n + E_m)$ include the repulsion from the negative-energy levels, while $E_k^{(|\nu|+1)\beta-1}$ includes the repulsion from the mirror level at $E_{\tilde{k}} = -E_k$ and from the zero modes. This modified repulsion follows again from the geometric argument above, where the subspace to be explored by the rotations $R^{(nm)}$ corresponds to the case $M_1 = |\nu| + 1$, $M_2 = 1$. In this space, A becomes a vector and the eigenvalues and the squared eigenvalues $E_n^2 = E_{\tilde{n}}^2 = |A|^2$ obey a χ^2 distribution.

These modifications affect the eigenvalue density around $E = 0$ over a range of a few level spacings,

$$\rho(E) - |\nu|\delta(E) \propto |E|^{(|\nu|+1)\beta-1} \quad \text{for small } |E|, \tag{2.6}$$

which now becomes a universal spectral characteristic of the system. For a macroscopic number of zero modes with $M_2 \gg M_1 \gg 1$, the repulsion yields a hard gap around the symmetry point, corresponding to the mean density

$$\rho(E) = \frac{\pi}{M_1 \Delta^2 E} \sqrt{(E^2 - E_-^2)(E_+^2 - E^2)}, \quad E_\pm = \frac{M_1 \Delta}{\pi} (\sqrt{M_2/M_1} \pm 1) \tag{2.7}$$

for the M_1 positive eigenvalues (this expression follows from the Marchenko-Pastur law derived in the Appendix). For $M_1 = M_2 \gg 1$ this eigenvalue density reverts to a Wigner semicircle law (2.3), normalised to $2M_1$ eigenvalues in the whole energy range (the level repulsion (2.6) is not resolved as in this limit $\Delta \to 0$).

2.1.3 Charge-conjugation symmetry

If we admit for an antisymmetry $\mathcal{C}\mathcal{H}\mathcal{C}^{-1} = -\mathcal{H}$ with an antiunitary operator $\mathcal{C}$ we encounter four additional cases (Altland and Zirnbauer, 1997). Two of these arise from the choices $\mathcal{C}^2 = \pm 1$, while the other two arise from an additional time-reversal symmetry with $\mathcal{T}^2 = -\mathcal{C}^2$.

If the antisymmetry is $\mathcal{C} = K$ ($\beta = \beta' = 2$), the Hamiltonian is imaginary and antisymmetric, $H = -H^* = -H^T$, and can be written in terms of matrix elements $H_{nm} \in i\mathbb{R}$. It is useful to denote this as the *real symmetry class* (RE) (Beenakker, 2015). If we have in addition a time-reversal symmetry $\mathcal{T} = \Omega K$ ($\beta = 4$, $\beta' = 3$) we can write the Hamiltonian in the block form

$$H = \begin{pmatrix} A & B \\ B & -A \end{pmatrix}, \tag{2.8}$$

where $A = -A^T$, $B = -B^T$ are antisymmetric and $A_{nm}, B_{nm} \in i\mathbb{R}$. This can be usefully denoted as the *time-invariant real symmetry class* (T-RE).

For the antisymmetry $\mathcal{C} = \Omega K$ ($\beta = 2$, $\beta' = 0$) the Hamiltonian $\overline{H} = -H$ is anti-selfconjugate, and thus can be written in terms of matrix elements $H_{nm} \in i\mathbb{H}$. If in addition we also have the time-reversal symmetry $T = K$ ($\beta = 1$, $\beta' = 0$), the Hamiltonian takes the block form (2.8) with symmetric matrices $A = A^T$, $B = B^T$ and elements $A_{nm}, B_{nm} \in \mathbb{R}$. The two cases define the *quaternion symmetry class* (QE) and the *time-invariant quaternion symmetry class* (T-QE)

In the two classes with $\mathcal{C}^2 = 1$, where the Hamiltonian can be made anti-symmetric by an appropriate basis choice, a topologically protected zero mode exists if M is odd (when we have an additional time-reversal symmetry with $\mathcal{T}^2 = -1$ this mode is Kramers-degenerate). The topological invariant counting such modes is then set to $\nu = 1$, while for even M we set $\nu = 0$. No such symmetry-protected zero modes exist in the two classes with $\mathcal{C}^2 = -1$.

Adopting again a Gaussian distribution $P(H) \propto \exp[-(c_\beta/2)\,\mathrm{tr}\, H^2]$ of matrix elements, these symmetry classes provide the joint probability density

$$P(\{E_n\}) \propto \prod_{n<m, E_{n,m}>0} |E_n^2 - E_m^2|^\beta \prod_{k, E_k>0} E_k^{(|\nu|+1)\beta-\beta'} \exp(-c_\beta E_k^2), \tag{2.9}$$

where β' modifies the repulsion from the mirror level as specified above (this follows again from the geometric argument in the small subspaces spanned by a level pair and any zero modes). As in the chiral classes, the spectral symmetry and the zero mode thus directly affect the level statistics in the closed system.

The symmetry associated with $\mathcal{C}$ is known as a charge-conjugation or particle-hole symmetry, and arises naturally in the context of superconducting systems. In a mean-field description, excitations are described as quasi-particles that obey the Boguliubov-de Gennes Hamiltonian

$$\mathcal{H} = \begin{pmatrix} H_0 - E_F & -i\sigma_y \otimes \Delta \\ i\sigma_y \otimes \Delta^* & E_F - H_0^* \end{pmatrix}, \tag{2.10}$$

where the blocks refer to the electron-like and hole-like degrees of freedom (addressed by Pauli matrices τ_i), the Pauli matrix σ_y acts in spin space, and $\Delta = \Delta^T$ is the

s-wave pair potential. The charge-conjugation is of the form $\mathcal{C} = \tau_x K$ and squares to $\mathcal{C}^2 = 1$. If $H_0 = H_+ \oplus H_-$ and $\Delta = \Delta_+ \oplus \Delta_-$ preserve the spin we can rearrange the Hamiltonian into two systems with $\mathcal{H}_\pm = \begin{pmatrix} H_\pm - E_F & \mp\Delta_\pm \\ \mp\Delta_\pm^* & E_F - H_\pm^* \end{pmatrix}$, for which the charge-conjugation symmetry $\mathcal{C} = \Omega K$ with $\Omega = i\tau_y$ squares to $\mathcal{C}^2 = -1$.

In this setting, the zero modes in the classes with $\mathcal{C}^2 = 1$ are associated with Majorana fermions (Alicea, 2012; Leijnse and Flensberg, 2012; Beenakker, 2013), previously elusive quasi-particles with possible applications for topological quantum computation (Nayak *et al.*, 2008). These concepts can be generalised to surface and interface states in systems of specified spatial dimensions (Kitaev, 2009; Teo and Kane, 2010; Ryu *et al.*, 2010), which are encountered in topological insulators and superconductors (Hasan and Kane, 2010; Qi and Zhang, 2011).

2.2 Random time-evolution operators and circular ensembles

To prepare how these considerations about the Hamiltonian translate to open systems, it is useful to turn to the dynamics and identify the corresponding symmetry classes of unitary matrices that exemplify the time evolution in the system. Of particular interest is the time evolution over a fixed time interval T_0, which also admits situations in which the Hamiltonian is itself time-dependent with that period. With a nod to the notion of a Floquet-operator in the latter setting, we denote this stroboscopic time-evolution operator over a fixed time interval as F. Its eigenvalues $z_n = \exp(-i\varepsilon_n)$ lie on the unit circle, where the phases ε_n can be interpreted as quasi-energies. Similar considerations apply to quantum maps (Haake, 2010) and quantum walks (Kitagawa *et al.*, 2010).

As the time evolution is generated by the Schrödinger equation (1.1), we can symbolically write $F = \exp(-iHT_0/\hbar)$ with a suitable effective Hamiltonian H. The symmetries of F then follow from the symmetries of H, and thus comply with the ten symmetry classes described above (Zirnbauer, 1996). In the resulting spaces of unitary matrices, some segments are smoothly connected to the identity, while others form disconnected pieces. This once more provides scope for topological invariants (Fulga *et al.*, 2011; Beenakker, 2015), which we specify in the following explicit constructions.

For the time-evolution operator, time-reversal symmetry implies $\mathcal{T}F\mathcal{T}^{-1} = F^{-1}$. Given a time-reversal symmetry with $\mathcal{T}^2 = 1$ (orthogonal symmetry class with $\beta = 1$) and adopting a canonical basis where this is represented by $\mathcal{T} = K$, we find that F is symmetric under transposition, $F = F^T$. In absence of any symmetries (unitary symmetry class with $\beta = 2$), F is only constrained by $F^{-1} = F^\dagger$, so a member of the unitary group $\mathrm{U}(M)$. For time-reversal symmetry with $\mathcal{T}^2 = -1$ (symplectic symmetry class with $\beta = 4$), the choice $\mathcal{T} = \Omega K$ implies that $F = \overline{F}$ is quaternion self-conjugate. The matrix $F_\Omega = \Omega F$ with elements $F_{\Omega,nm} = i\sigma_y F_{nm}$, written as a normal $2M \times 2M$ matrix, is then antisymmetric, $F_\Omega^T = -F_\Omega$. Notably, in the two classes arising from time-reversal symmetry, even though denoted as orthogonal and symplectic, the spaces of matrices differ from the groups of orthogonal and symplectic matrices encountered in the diagonalisation of the corresponding Hamiltonians. Only in the case of broken time reversal symmetry the space remains associated with the unitary group.

In each of these three spaces we can again determine a Haar measure $\mu(F)$. This is uniquely defined by the requirement that the measure is invariant under transfor-

mations $F \to U'FU$, but now with unitary matrices U, U' that are subject to the constraints $U' = U^T$ in the orthogonal symmetry class, and $U' = \overline{U}$ in the symplectic symmetry class. Equipped with this measure, the corresponding ensembles are known as the circular ensembles (COE, CUE and CSE) (Dyson, 1962*a*). The joint distributions of phases φ_n in the unimodular eigenvalues $z_n = e^{i\varphi_n}$ is given by

$$P(\{\varphi_n\}) \propto \prod_{n<m} |e^{i\varphi_n} - e^{i\varphi_m}|^\beta, \tag{2.11}$$

and their density is uniform.

Chiral symmetry implies $\mathcal{X}F\mathcal{X} = F^\dagger$, so that $F_X = \mathcal{X}F$ is hermitian and only has eigenvalues ± 1. A topological invariant can then be defined as $\nu' = \frac{1}{2}\mathrm{tr}\,(F_X) = (M_+ - M_-)/2$, where $M_\pm$ counts the eigenvalues of either sign. One can again introduce a Haar measure, which in combination with the possible constraints from time-reversal symmetry leads to three chiral circular ensembles (chCOE, chCUE and chCSE).

A charge-conjugation symmetry implies $\mathcal{C}F\mathcal{C}^{-1} = F$. When we express $\mathcal{C} = K$ with $\mathcal{C}^2 = 1$ this implies that $F = F^*$ is real, and thus an element of the orthogonal group $\mathrm{O}(M)$ (as the label OE is already taken this justifies the notion of the real symmetry class RE). We then have the invariant $\nu' = \det F$, where $\nu' = 1$ accounts for matrices from $\mathrm{SO}(M)$. If in addition we have a time-reversal symmetry with $\mathcal{T} = K\Omega$ (class T-RE), such an invariant can be formulated with help of the Pfaffian $\nu' = \mathrm{pf}F_\Omega$ of the real antisymmetric matrix $F_\Omega = \Omega F$. For $\mathcal{C} = \Omega K$ with $\mathcal{C}^2 = -1$, the constraint can be written as $F^T\Omega F = \Omega$, which identifies F as symplectic (in quaternion language, $F\overline{F} = 1$, which justifies the notion of the quanternion universality class QE). If in addition we have a time-reversal symmetry with $\mathcal{T} = K$ (class T-QE), the matrix is furthermore constrained to be symmetric. Equipped with a Haar measure, the corresponding real and quaternion circular ensembles are denoted as CRE, T-CRE, CQE and T-CQE (Beenakker, 2015).

In a specific mathematical sense, it can now be argued that these ten classes provide a complete classification of random-matrix ensembles (Zirnbauer, 1996; Caselle and

Table 2.2 Classification of unitary matrix ensembles

symmetries	unitary matrices	space	Cartan label
no symmetries	$F^{-1} = F^\dagger$	$\mathrm{U}(M)$	A
$\mathcal{T} = K$	$F^{-1} = F^*$	$\mathrm{U}(M)/\mathrm{O}(M)$	AI
$\mathcal{T} = \Omega K$	$F^{-1} = \Omega F^*\Omega^{-1}$	$\mathrm{U}(2M)/\mathrm{Sp}(2M)$	AII
$\mathcal{C} = K$	$F^{-1} = F^T$	$\mathrm{O}(M)$	D
$\mathcal{C} = K$, $\mathcal{T} = \Omega K$	$F^{-1} = F^T = \Omega F\Omega^{-1}$	$\mathrm{O}(2M)/\mathrm{U}(M)$	DIII
$\mathcal{C} = \Omega K$	$F^{-1} = \Omega F^T\Omega^{-1}$	$\mathrm{Sp}(2M)$	C
$\mathcal{C} = \Omega K$, $\mathcal{T} = K$	$F^{-1} = F^* = \Omega F\Omega^{-1}$	$\mathrm{Sp}(2M)/\mathrm{U}(M)$	CI
$\mathcal{X} = \tau_z$	$(\mathcal{X}F) = (\mathcal{X}F)^\dagger$	$\mathrm{U}(M_1 + M_2)/\mathrm{U}(M_1) \otimes \mathrm{U}(M_2)$	AIII
$\mathcal{X} = \tau_z$, $\mathcal{C} = K$	$(\mathcal{X}F) = (\mathcal{X}F)^T = (\mathcal{X}F)^*$	$\mathrm{O}(M_1 + M_2)/\mathrm{O}(M_1) \otimes \mathrm{O}(M_2)$	BDI
$\mathcal{X} = \tau_z$, $\mathcal{C} = \Omega K$	$(\mathcal{X}F) = (\mathcal{X}F)^\dagger = \Omega(\mathcal{X}F)^*\Omega^{-1}$	$\mathrm{Sp}(2M_1 + 2M_2)/\mathrm{Sp}(2M_1) \otimes \mathrm{Sp}(2M_2)$	CII

Magnea, 2004; Zirnbauer, 2011)—they arise from the groups of unitary, orthogonal and symplectic matrices and the associated compact symmetric Riemannian spaces, as classified by Cartan and summarised in Table 2.2. The three Wigner-Dyson classes with unitary, orthogonal and sympletic symmetry (UE, OE and SE) are the labelled A, AI, AII; the corresponding chiral classes (chUE, chOE and chSE) are labelled AIII, BDI, CII; the classes with charge-conjugation symmetry $\mathcal{C}^2 = 1$ and topological invariants (RE and T-RE) are labelled D and DIII, while the remaining to classes with $\mathcal{C}^2 = -1$ (QE and T-QE) are labelled C and CI.

2.3 Positive-definite matrices and Wishart-Laguerre ensembles

As we have seen in the construction of the ten Hamiltonian ensembles, it is often useful to study the blocks of a matrix, and compose new matrices out from them. This leads to natural extensions of the ensembles encountered so far, which can be justified via their connection to orthogonal polynomials (Mehta, 2004; Forrester, 2010). From this perspective, the Gaussian hermitian matrix ensembles in the Wigner-Dyson classes are related to Hermite polynomials, while the other ensembles are related to Laguerre polynomials. As mentioned for the chiral symmetry classes, these ensembles are naturally related to positive semidefinite matrices $W = X^\dagger X$, where X is an $M' \times M$-dimensional matrix. It suffices to consider the case $M \leq M'$, as otherwise we can simply study $W = XX^\dagger$.

We again use the symmetry index $\beta = 1, 2, 4$ to distinguish settings where the matrix elements X_{lm} are real, complex or quaternion. A Gaussian distribution

$$P(X) \propto \exp(-c'_\beta \operatorname{tr} X^\dagger X) \tag{2.12}$$

then defines the Wishart-Laguerre ensemble for W, where we set $c'_\beta = \beta/2\sigma^2$. This ensemble was first introduced by Wishart (1928) in the context of multivariate statistics, which marks the historical beginnings of random-matrix applications. The joint probability density of the eigenvalues λ of W is given by

$$P(\{\lambda_n\}) \propto \prod_{n<m} |\lambda_n - \lambda_m|^\beta \prod_k \lambda_k^{\beta(1+M'-M)/2-1} \exp(-c'_\beta \lambda_k), \tag{2.13}$$

which relates to the previously encountered eigenvalue distributions by the substitution $\lambda_n = E_n^2$. As mentioned above, the resulting eigenvalue correlations can be expressed in terms of Laguerre polynomials.

For large matrix dimensions the eigenvalue density approaches the Marchenko-Pastur law (Marčenko and Pastur, 1967)

$$\rho(\lambda) = \frac{MT_0}{2\pi\lambda} \sqrt{(\lambda - \lambda_-)(\lambda_+ - \lambda)} \quad \text{for } \lambda_- < \lambda < \lambda_+, \tag{2.14}$$

where $\lambda_\pm = (\sqrt{M'} \pm \sqrt{M})^2/\sigma^2$ defines the range where this density is finite. This expression is derived in the Appendix.

2.4 Jacobi ensembles

A third class of classical orthogonal polynomials appearing in random-matrix problems are the Jacobi polynomials. These are associated with joint probability distributions of the form (Forrester, 2010)

$$P(\{\mu_n\}) \propto \prod_{n<m} |\mu_n - \mu_m|^\beta \prod_k (1-\mu_k)^{a\beta/2}(1+\mu_k)^{b\beta/2}, \tag{2.15}$$

where $\mu_m \in [-1,1]$, $m = 1,2,3,\ldots,M$.

Such distributions arise, for instance, when one considers the singular values of an $M' \times M$ dimensional off-diagonal block t of a suitable $N \times N$ dimensional unitary matrix F (Beenakker, 1997; Beenakker, 2015). In particular, setting $N = M+M'$ with $M' \geq M$ and generating F from the three standard circular ensembles (COE, CUE or CSE), the eigenvalues $T_n = (1-\mu_n)/2 \in [0,1]$ of $t^\dagger t$ obey a Jacobi ensemble with $a = M'-M+1-2/\beta$, $b = 0$; similarly, if F is taken from $\mathrm{O}(M+M')$ or $\mathrm{Sp}(2M+2M')$ (symmetry class D or C) one finds the same a but $b = 1-2/\beta$; the complete picture is presented in Section 4.4.

Alternatively (Forrester, 2010), the quantities T_n can be interpreted as the eigenvalues of a so-called MANOVA matrix $(X^\dagger X + Y^\dagger Y)^{-1} X^\dagger X$, where X and Y are matrices of dimensions $M_x \times M$ and $M_y \times M$, distributed as Gaussians with equal variance σ according to Eq. (2.12). In this case, $a = M_x - M + 1 - 2/\beta$, $b = M_y - M + 1 - 2/\beta$. As shown based on this realization in the Appendix, in the limit of a large matrix dimension M with fixed $c_x = M_x/M$, $c_y = M_y/M$ the eigenvalue density approaches

$$\rho(T) = \frac{M(c_x+c_y)\sqrt{(T-T_-)(T_+-T)}}{2\pi T(1-T)}, \tag{2.16}$$

where

$$T_\pm = \frac{1}{1+\lambda_\mp}, \quad \lambda_\pm = \left(\frac{\sqrt{c_x c_y} \pm \sqrt{c_x+c_y-1}}{c_x-1}\right)^2 \tag{2.17}$$

determines the range where the density is finite. In terms of the variables μ_n, this takes the form

$$\rho(\mu) = \frac{M(c_x+c_y)}{2\pi} \frac{\sqrt{(\mu-\mu_-)(\mu_+-\mu)}}{1-\mu^2}, \tag{2.18}$$

within the boundaries given by $\mu_\pm = (\lambda_\pm - 1)/(\lambda_\pm + 1)$.

2.5 Non-hermitian matrices

The eigenvalues λ_n in the Wishart matrix $W = X^\dagger X$ are the squared singular values of the matrix X. For a square matrix of dimensions $M \times M$ we can also study the complex eigenvalues z_n of X, obtained from $X\mathbf{v}_n = z_n \mathbf{v}_n$ with eigenvectors $\mathbf{v}_n$. This leads to entirely different classes of random matrices (Ginibre, 1965; Khoruzhenko and Sommers, 2011). Since X is in general not normal (in particular neither hermitian nor unitary), there is no direct relation between the real singular values and the complex eigenvalues z_n. This key difference is intimately related to the fact that the eigenvectors

$\mathbf{v}_n$ are not orthogonal to each other, so that the spectral decomposition $X = VDV^{-1}$ with $D = \mathrm{diag}(z_n)$ involves a non-unitary matrix V. We therefore need to distinguish the right eigenvectors $\mathbf{v}_n$, which form the columns of V, from the left eigenvectors $\mathbf{w}_n$, which are obtained from $\mathbf{w}_n X = s_n \mathbf{w}_n$. Imposing the biorthogonality condition $\mathbf{w}_m \mathbf{v}_n = \delta_{nm}$, the left eigenvectors form the rows of V^{-1}.

This biorthogonal set of eigenvectors is in general no longer normalised. The extent of mode non-orthogonality can thus be quantified by the condition numbers (Chalker and Mehlig, 1998; Janik *et al.*, 1999; Schomerus *et al.*, 2000)

$$O_{mn} = \frac{(\mathbf{v}_m^\dagger \mathbf{v}_n)(\mathbf{w}_n \mathbf{w}_m^\dagger)}{(\mathbf{v}_m^\dagger \mathbf{w}_m^\dagger)(\mathbf{w}_n \mathbf{v}_n)}, \tag{2.19}$$

which we have written in a way that does not rely on the chosen normalisation condition. In terms of the matrix V,

$$O_{mn} = (V^\dagger V)_{mn} (V^{-1} V^{-1\dagger})_{nm}. \tag{2.20}$$

The diagonal elements $K_m = O_{mm}$ are real and obey $K_m \geq 1$, with $K_m = 1$ for all m only if V is unitary. These quantities become large in particular when two eigenvalues approach each other closely, and indeed diverge at eigenvalue degeneracies, so-called exceptional points (Berry, 2004; Heiss, 2012). Close to such a degeneracy with a coalescing pair $z_{n+1} = z_n$, X cannot be diagonalised but only be brought into a form involving Jordan blocks

$$\begin{pmatrix} z_n & 1 \\ 0 & z_n \end{pmatrix}. \tag{2.21}$$

This means that the eigenvectors of the modes become identical, in sharp contrast to hermitian systems where the eigenvectors remain orthogonal as one approaches a degeneracy.

The probability distribution (2.12) for $M \times M$-dimensional square matrices X defines the Ginibre ensemble (Ginibre, 1965; Khoruzhenko and Sommers, 2011). For the complex Ginibre ensemble ($\beta = 2$), the joint distribution of eigenvalues is

$$P(\{z_n\}) \propto \prod_{n<m} |z_n - z_m|^2 \prod_k \exp(-c'_\beta z_k^2). \tag{2.22}$$

In the quaternion case $\beta = 4$ eigenvalues come in conjugate pairs, and the joint distribution of eigenvalues in the upper half of the complex plane

$$P(\{z_n\}) \propto \prod_{n<m} |z_n - z_m|^2 |z_n - z_m^*|^2 \prod_k |z_k - z_k^*|^2 \exp(-c'_\beta z_k^2) \tag{2.23}$$

contains the expected self-repulsion terms. For the real case $\beta = 1$, much more complicated expressions arise due to the accumulation of $O(\sqrt{M})$ eigenvalues on the real axis (Lehmann and Sommers, 1991; Forrester and Nagao, 2007). What is common to all three cases are the local spectral correlations of eigenvalues well inside the complex support (away from the boundaries and spectral symmetry lines), which irrespective of β are determined by the factors $|z_n - z_m|^2$. This yields a cubic level repulsion $P(s) \propto s^3$

for small spacings $s = |z_n - z_m|$, where one power of s arises from the area element in the complex plane.

As shown in the Appendix for the complex Ginibre ensemble, for a variance scaled to $\sigma^2 = 1/M$ and $M \to \infty$ the eigenvalue density in the complex plane approaches Ginibre's circular law $\rho(z) = \frac{M}{\pi}\Theta(1 - |z|)$, where Θ denotes the unit step function. As a side product of the calculation presented there (Janik *et al.*, 1999), the condition number $\overline{K_m}|_{z_m=z} \sim M(1 - |z|^2)$ turns out to be large, unless one approaches the boundaries of the eigenvalue support.

From the general perspective of commutation and anticommutation with unitary and anti-unitary symmetries, non-hermitian matrices admit a very large number of symmetry classes (Magnea, 2008). For a physical setting that illustrates this richness, we can consider photonic systems with absorption and amplification (Cao and Wiersig, 2015). Without further constraints we may model these as a complex Ginibre ensemble ($\beta = 2$) with different weights of the hermitian and non-hermitian contributions, where the eigenvalue support becomes elliptic (Girko, 1986). Time-reversal symmetry in optics (reciprocity) makes the matrix complex symmetric, $H = H^T \neq H^*$, which modifies the statistics but does not entail any spectral constraints. As a template for the real Ginibre ensemble ($\beta = 1$), we can take a system with balanced amplification and absorption, situated in regions that are mapped onto each other by a reflection or inversion P (Makris *et al.*, 2008; Rüter *et al.*, 2010). We then obtain a non-hermitian PT-symmetric system with $PHP = H^* \neq H^T$ (Bender, 2007), which in a suitable basis is represented by a real asymmetric matrix. In combination with magneto-optical effects, we can similarly construct PTT′-symmetric systems with $PHP = H^\dagger \neq H$ (Schomerus, 2013*a*). The spectrum remains symmetric about the real axis, and a random-matrix analysis reveals a close connection to the real Ginibre ensemble, including the same accumulation of $O(\sqrt{M})$ eigenvalues on the real axis (Birchall and Schomerus, 2012). Further examples can be constructed by modifying the role of P. In an optical system where P represents a chiral symmetry, we can realize the case $H = -PH^*P$ in which eigenvalues are symmetric with respect to the imaginary axis (Schomerus and Halpern, 2013; Schomerus, 2013*b*; Poli *et al.*, 2015), as well as the case $H = H^* = -PHP$ in which eigenvalues are symmetric with respect to both the real and the imaginary axis (Malzard *et al.*, 2015). For a symmetry with $P^2 = -1$ (hence $P = -P^T$, assuming P is real), two interesting cases are the so-called Hamiltonian ensembles with $PHP = H^T$, as well as the skew-Hamiltonian ensembles with $PHP = -H^T$ (these notions relate to the symplectic structure of classical Hamiltonians, generated by an antisymmetric involution such as P; Beenakker *et al.* 2013). For a real Hamiltonian matrix with Gaussian statistics, $O(\sqrt{M})$ eigenvalues accumulate both on the real and on the imaginary axis; for a real skew-Hamiltonian matrix, all eigenvalues are twofold degenerate and $O(\sqrt{M})$ of these pairs accumulate on the real axis.

In the next Chapter we will see that non-hermitian matrices play a crucial role in the description of open scattering systems, where additional constraints arise from the physical constraints of unitarity and causality.

3
The scattering matrix

In this chapter we develop effective models for the scattering matrix and use these to identify the associated random-matrix ensembles.

3.1 Points of interest

Consider a particle moving through a scattering region with a spatially varying potential energy V, as sketched for a simple one-dimensional setting in Fig. 3.1. The corresponding Hamiltonian is $\hat{H} = \hat{T} + \hat{V}$, where $\hat{T}$ represents the kinetic energy. Here are some natural phenomena that we may wish to consider: Decay, where we address the escape rate of a particle inserted into the scattering region; transport, where we address the probability for an incident particle to be transmitted or reflected; dynamics, where we ask how long the particle engages with the scattering region and how many internal states it explores. We may also wish to identify system-specific details beyond the fundamental symmetries, such as regarding the role of different scattering

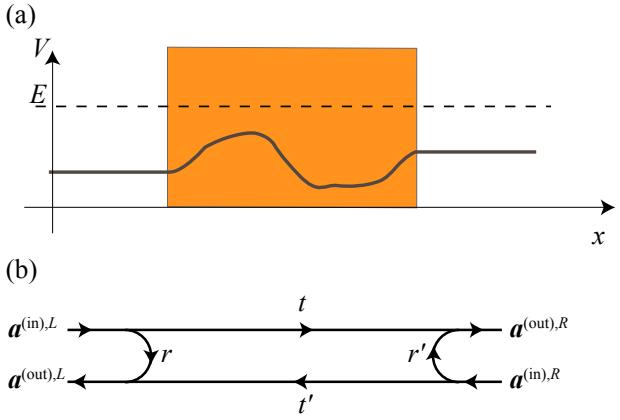

Fig. 3.1 (a) Sketch of a scattering region with a varying potential $V(x)$ in a one-dimensional system, with ideal leads attached to either side. Note that the potential does not need to be identical in both leads. (b) Scattering processes relating the amplitudes of propagating waves in the leads.

subregions or the role of the contacts. All of these questions (and many more) can be addressed with the help of a single object, the scattering matrix $S(E)$.

3.2 Definition of the scattering matrix

To define the scattering matrix (Newton, 2002; Messiah, 2014) we stipulate that the motion outside the scattering region is ballistic. At any energy E, we then have access to a complete set of propagating scattering states $|\psi_n^{(\mathrm{in})}\rangle$ in which the particle is approaching the scattering region (incoming channels), and a corresponding set of propagating states $|\psi_n^{(\mathrm{out})}\rangle$ where the particle is moving away from the region (outgoing channels). These states are taken to be normalised to a unit probability flux through any closed surface surrounding the scattering region. We may also encounter a set of non-propagating (evanescent) states $|\psi_m^{(\mathrm{ev})}\rangle$ which decay away from the scattering region and do not carry any flux. Outside the scattering region, we then can write a state with a given energy as

$$|\psi\rangle = \sum_{n=1}^{N} a_n^{(\mathrm{in})} |\psi_n^{(\mathrm{in})}\rangle + \sum_{n=1}^{N} a_n^{(\mathrm{out})} |\psi_n^{(\mathrm{out})}\rangle + \sum_l a_l^{(\mathrm{ev})} |\psi_m^{(\mathrm{ev})}\rangle, \tag{3.1}$$

where N fixes the number of scattering channels. We collect the expansion coefficients into vectors $\mathbf{a}^{(\mathrm{in})}$, $\mathbf{a}^{(\mathrm{out})}$ and $\mathbf{a}^{(\mathrm{ev})}$.

Inside the scattering region, we may expand the state in terms of any suitable complete set of modes, $|\psi\rangle = \sum_m b_m |\chi_m\rangle$ with a coefficient vector $\mathbf{b}$. With help of the stationary Schrödinger equation (1.1), the states inside and outside the scattering region are uniquely related. In particular, if we fix $\mathbf{a}^{(\mathrm{in})}$ then the solution of the Schrödinger equation uniquely fixes $\mathbf{a}^{(\mathrm{out})}$, $\mathbf{a}^{(\mathrm{ev})}$, and $\mathbf{b}$, up to effectively decoupled parts that can be treated as a separate system. These relations must be linear, so that

$$\mathbf{a}^{(\mathrm{out})} = S(E)\mathbf{a}^{(\mathrm{in})}. \tag{3.2}$$

This defines the scattering matrix. Flux normalization ensures that for real energies $S(E)$ is unitary, hence $S(E) \in \mathrm{U}(N)$. Causality ensures that the poles E_l of S at complex energies are all confined to the lower half of the complex plane, $\operatorname{Im} E_l < 0$. The number of propagating scattering channels N may change at certain energies, which gives rise to branch cuts in the complex-energy plane.

3.3 Preliminary answers

The scattering matrix addresses the phenomena listed at the beginning of this chapter in the following ways.

Decay.—The complex poles $E_l = E_l' - i\hbar\gamma_l/2$ of the scattering matrix provide solutions where $\mathbf{a}^{(\mathrm{out})}$ is finite while $\mathbf{a}^{(\mathrm{in})} = 0$. These quasi-bound states provide a fundamental description of decay and resonant scattering (Guhr *et al.*, 1998; Weidenmüller and Mitchell, 2009; Moiseyev, 2011). The time dependence of the quasibound states follows from the amplitude factor $A(t) = \exp(-itE_l/\hbar) = \exp(-itE_l'/\hbar)\exp(-t\gamma_l/2)$,

so that the corresponding intensity $|A(t)|^2 = \exp(-t\gamma_l)$ decays with rate γ_l. For a particle prepared in this state at $t = 0$, the Fourier signal

$$A(\omega) = \int_0^\infty A(t)e^{i\omega t}\, dt = i[(\omega - E_l'/\hbar) + i\gamma_l/2]^{-1} \tag{3.3}$$

delivers the resonance-like frequency-resolved signal

$$|A(\omega)|^2 = \frac{1}{(\omega - E_l'/\hbar)^2 + \gamma_l^2/4}, \tag{3.4}$$

a Lorentzian centred at $E_l'/\hbar$ with full width at half maximum γ_l. When the particle is prepared in a superposition of quasi-bound states, the resulting decay for long times depends on the characteristic decay rate $\gamma_0 = \inf \gamma_l$, defined such that $\gamma_l \geq \gamma_0$ for all contributing states. If $\gamma_0 > 0$ the decay becomes exponential, while for $\gamma_0 = 0$ one typically encounters a power-law.

Transport.—For a particle incoming in channel n, the probability to scatter into the outgoing channel n' is given by $|S_{n'n}|^2$. The unitarity of the scattering matrix guarantees that the sums of probabilities $\sum_n |S_{n'n}|^2 = \sum_{n'} |S_{n'n}|^2 = 1$ are normalised. This normalization also holds for an incident particle in any superposition of incoming modes, $|\mathbf{a}^{(\mathrm{out})}|^2 = |\mathbf{a}^{(\mathrm{in})}|^2$. These features are at the heart of the scattering approach to transport (Beenakker, 1997; Blanter and Büttiker, 2000; Nazarov and Blanter, 2009).

In many settings, we are let to group the scattering amplitudes into subcomponents $\mathbf{a}^{(\mathrm{in}),\mathrm{s}}$, $\mathbf{a}^{(\mathrm{out}),\mathrm{s}}$, where s labels different asymptotic regions (leads). The scattering matrix is then formed of blocks $S_{s's}$ describing transmission from lead s to lead s', and reflections back into lead s if $s' = s$. The associated transmission probability is quantified by the dimensionless conductance $g_{s's} = \mathrm{tr}\,(S_{s's}^\dagger S_{s's})$. In the case of two leads, designated as a left lead $s = L$ with N_L channels and a right lead $s = R$ with N_R channels, we write the blocks as

$$S = \begin{pmatrix} r & t' \\ t & r' \end{pmatrix}, \tag{3.5}$$

where r and t describe the reflection and transmission of particles arriving from the left, while r' and t' describe these processes for particles arriving from the right. This designation is illustrated in Fig. 3.1(b). The dimensionless conductance is then given by $g = \mathrm{tr}\, t^\dagger t = \mathrm{tr}\, t'^\dagger t' = N_L - \mathrm{tr}\, r^\dagger r = N_R - \mathrm{tr}\, r'^\dagger r'$, where the stated identities follow from unitarity.

The eigenvalues $T_n \in [0, 1]$ of the hermitian matrix $t^\dagger t$ are known as the transmission eigenvalues, and determine the dimensionless conductance via $g = \sum_n T_n$. The quantities $\sqrt{T_n}$ can be interpreted as the singular values of t, which generalises to the polar decomposition of the scattering matrix,

$$S = \begin{pmatrix} V & 0 \\ 0 & V' \end{pmatrix} \begin{pmatrix} \sqrt{1-T} & \sqrt{T} \\ \sqrt{T} & -\sqrt{1-T} \end{pmatrix} \begin{pmatrix} V'' & 0 \\ 0 & V''' \end{pmatrix}, \quad T = \mathrm{diag}\,(T_n) \tag{3.6}$$

with unitary matrices V, V', V'' and V'''.

The transmission eigenvalues determine many other transport properties, including the full counting statistics of electrons at low temperatures (Levitov and Lesovik, 1993), with the shot noise characterised by the second binomial cumulant (Büttiker, 1990; Blanter and Büttiker, 2000)

$$\sum_n T_n(1-T_n). \tag{3.7}$$

Another example is the charge transport through a normal conductor into a conventional superconducting lead (Beenakker, 1992; Beenakker, 1997), for which the dimensionless conductance at vanishing magnetic fields is given by

$$g_{NS} = \sum_n T_n^2/(2-T_n)^2. \tag{3.8}$$

Dynamics.—Complementing the information about the scattering probabilities, the phase φ of a scattering amplitude $S_{n'n} = |S_{n'n}|e^{i\varphi}$ provides insight into the dynamics (de Carvalho and Nussenzveig, 2002; Texier, 2016). For instance, for ballistic propagation through a region of length L at a constant momentum $p(E)$, the particle picks up the dynamical phase $\varphi = pL/\hbar$. The energy sensitivity $\hbar d\varphi/dE = L/v = \tau$ of the phase therefore gives an indication of the travel time. In a semiclassical description of scattering from a slowly varying potential, we have $\varphi = S_{\rm cl}/\hbar$, where the classical action $S_{\rm cl}$ again obeys $dS_{\rm cl}/dE = \tau$.

These observations lead to the formal definition of the delay time of a particle that passes through the scattering region. For injection and extraction in individual channels, the delay time can be isolated by the logarithmic derivative $\mathrm{Im}\, S^{-1}_{n'n} dS_{n'n}/dE$. For multi-channel scattering this is generalised by the Wigner-Smith time-delay matrix (Wigner, 1955; Smith, 1960)

$$Q = -i\hbar S^\dagger dS/dE. \tag{3.9}$$

The unitarity of S at any energy ensures that $Q = Q^\dagger$ is hermitian, while causality ensures that Q is positive semidefinite. Therefore, the eigenvalues τ_n of Q are real and positive. These eigenvalues are known as the proper delay times.

Noting that $v^{-1} = dp/dE$ also appears in semiclassical estimates of the accessible phase-space volume, the delay times are intimately related to the density of states. Indeed, the Wigner-Smith matrix directly quantifies the global density of states in the system, in terms of the Birman-Krein formula (Birman and Krein, 1962)

$$\rho(E) = \frac{1}{2\pi\hbar}\mathrm{tr}\, Q. \tag{3.10}$$

Replacing the derivative d/dE by a local variation of the potential $\partial/\partial V(x)$, this approach can be extended to obtain the local density of states (Gasparian *et al.*, 1996). Analogous variations with respect to other parameters deliver a wide range of response functions, which can for instance be used to study adiabatic transport and quantum pumping (Büttiker *et al.*, 1994; Brouwer, 1998).

System-specific details.—When we separate the scattering region into subregions, we can build up the total scattering matrix from the scattering problems of the subregions (Datta, 1997; Beenakker, 1997; Nazarov and Blanter, 2009). This can be done

exactly if we extend the scattering matrix to include evanescent states, and often still very reliably if we only account for the propagating states. The simple idea is to inspect each interface and identify the amplitudes of outgoing states from one region with the amplitudes of incoming states into the adjacent region.

For the case of two adjacent regions with scattering matrices S_1, S_2 of the form (3.5), the wave-matching of propagating states leads to the composition law

$$S_{1\oplus 2} = \begin{pmatrix} r_1 + t_1' r_2 (1 - r_1' r_2)^{-1} t_1 & t_1' (1 - r_2 r_1')^{-1} t_2' \\ t_2 (1 - r_1' r_2)^{-1} t_1 & r_2' + t_2 r_1' (1 - r_2 r_1')^{-1} t_2' \end{pmatrix}. \tag{3.11}$$

This rule can be reformulated as a simple matrix multiplication $M = M_2 M_1$ for the transfer matrix

$$M = \begin{pmatrix} t^{\dagger -1} & r' t'^{-1} \\ r'^{\dagger} t^{\dagger -1} & t'^{-1} \end{pmatrix}, \tag{3.12}$$

which relates modes on the left and right according to

$$\begin{pmatrix} \mathbf{a}^{\mathrm{out},R} \\ \mathbf{a}^{\mathrm{in},R} \end{pmatrix} = M \begin{pmatrix} \mathbf{a}^{\mathrm{in},L} \\ \mathbf{a}^{\mathrm{out},L} \end{pmatrix}. \tag{3.13}$$

Flux conservation translates to the property $M^\dagger \sigma_z M = \sigma_z$, so that M is complex symplectic. The eigenvalues of $M^\dagger M$ and $(M^\dagger M)^{-1} = \sigma_z M^\dagger M \sigma_z$ are thus identical and appear in reciprocal pairs, which are given by $(\sqrt{1/T_n} \pm \sqrt{-1 + 1/T_n})^2$.

We note that in the composed system, according to Eq. (3.11) poles from the multiple scattering across the interface arise from

$$\det[1 - r_2(E) r_1'(E)] = 0. \tag{3.14}$$

Similarly, the role of a contact can be studied by inserting a static tunnel barrier at the corresponding boundary of the scattering region (Brouwer, 1995; Beenakker, 1997). For example, the scattering matrix

$$S_B = \begin{pmatrix} \sqrt{1 - \Gamma^2} & \sqrt{\Gamma} \\ \sqrt{\Gamma} & -\sqrt{1 - \Gamma^2} \end{pmatrix} \tag{3.15}$$

describes a barrier with uniform transparency $\Gamma \in [0, 1]$ in all channels. If we send $\Gamma \to 0$ for all contacts the system becomes closed. Poles approaching the real axis become the energy levels of the closed system, while poles moving deep into the complex plane are associated with direct reflection processes from the outside.

We can also artificially separate a closed system into two open systems joined by an interface. For a left and a right region, this is described by scattering matrices $S_1 = r_1'$ and $S_2 = r_2$, both only composed of a reflection block back to the interface. The quantization condition (3.14) can then be rewritten as

$$\det\left(S_1(E) S_2(E) - 1\right) = 0, \tag{3.16}$$

which determines the energies of the closed systems. This scattering quantization approach becomes exact when one includes the evanescent modes into the scattering description (Doron and Smilansky, 1992; Bäcker, 2003), and can be extended, e.g., to superconducting systems (Beenakker, 2005) and non-hermitian photonic systems (Schomerus, 2013*a*).

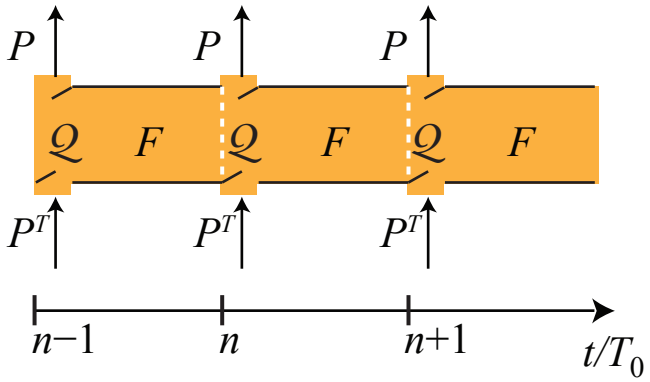

Fig. 3.2 Illustration of the stroboscopic scattering approach, in which particles are injected and collected at regular intervals.

3.4 Effective scattering models

In practice, many methods are available to calculate the scattering matrix in specific settings. This includes wave matching, Green function methods and the boundary integral method, as well as iterative procedures based on the composition rule (3.11) of scattering matrices, and analogous rules for the Green function (Datta, 1997). For the purpose of a statistical description, however, we require a generic model that captures the essential features of the internal dynamics and the coupling to the leads. This is delivered by the Mahaux-Weidenmüller formula (Mahaux and Weidenmüller, 1969; Livsic, 1973; Verbaarschot *et al.*, 1985; Guhr *et al.*, 1998)

$$S(E) = \frac{i\pi W^\dagger (E-H)^{-1} W - 1}{i\pi W^\dagger (E-H)^{-1} W + 1}, \tag{3.17}$$

where H is an effective internal Hamiltonian of dimension $M \times M$ while W is a suitable $M \times N$-dimensional coupling matrix, specified fully in Eq. (3.40).

We provide a motivation of this formula via a detour to the stroboscopic scattering problem (Fyodorov and Sommers, 2000; Tworzydło *et al.*, 2003), which leads to its close cousin

$$S(\varepsilon) = \frac{K\mathcal{A}K^T - 1}{K\mathcal{A}K^T + 1}, \quad \mathcal{A} = \frac{1 + e^{i\varepsilon}F}{1 - e^{i\varepsilon}F} = -\mathcal{A}^\dagger. \tag{3.18}$$

Here F is an effective internal time-evolution operator over a fixed time period T_0, ε is the associated quasi-energy, and the coupling matrix K is fully specified in (3.34). The Mahaux-Weidenmüller formula then follows in the continuum limit $T_0 \to 0$. We present this construction because it gives rather direct intuitive insight into scattering and decay problems, and also helps to isolate and justify the general features of the scattering matrix described in the previous section.

3.4.1 Stroboscopic scattering approach

Stroboscopic ballistic decay. Our starting point is a simple, highly idealised scenario, which nonetheless can be easily extended to capture a large range of other cases.

Consider a situation where the coupling of the scattering region to the outside occurs stroboscopically, at periodically spaced, discrete times $t = nT_0 \equiv t_n$, $n = 0, 1, 2, 3, \ldots$ (see Fig. 3.2). Let us denote the state within the system just before these times as $|\psi_n\rangle = |\psi(t_n^-)\rangle$. This state evolves stroboscopically according to

$$|\psi_n\rangle = F\mathcal{Q}|\psi_{n-1}\rangle = (F\mathcal{Q})^n|\psi_0\rangle, \tag{3.19}$$

where F is the unitary operator that describes the time evolution when the system is closed, while $\mathcal{Q}$ is a projector that describes what remains in the system when the system is open. In other words, in each time interval, we lose some internal wave amplitude according to the complementary projector $\mathcal{P} = 1 - \mathcal{Q}$, while the remaining amplitude is propagated by the unitary time evolution operator F. As we assume that F and $\mathcal{Q}$ are independent of the time index n, we require that the details of the coupling are otherwise time-independent and the internal dynamics are autonomous, or at least themselves time-periodic with period T_0. The fact that we take $\mathcal{Q}$ as a projector means that the coupling is *ballistic*—the opening is fully transparent, without any partial reflection of the passing wave. This is also called an ideal lead.

According to Eq. (3.19), the decay of the amplitude within this system is described by the non-unitary operator $F\mathcal{Q}$. In a basis where $\mathcal{Q}$ is diagonal this corresponds to *truncating* the unitary operator F. Let us specify this for a system with a finite internal Hilbert space of dimension M, coupled to N external channels such that $\operatorname{rank}\mathcal{Q} = M - N$. In the basis where $\mathcal{Q} = \operatorname{diag}(0, 0, 0, \ldots, 0, 1, 1, \ldots, 1)$ (N zeros followed by $M - N$ ones), $F\mathcal{Q}$ is then obtained from F by setting the first N columns to zero.

In this setting, the quasibound states $|\phi_m\rangle$ are obtained from the eigenvalue problem

$$F\mathcal{Q}|\phi_m\rangle = z_m|\phi_m\rangle, \quad = 1, 2, \ldots, M. \tag{3.20}$$

Due to the projective nature of $\mathcal{Q}$, there will by N vanishing eigenvalues, while the remaining eigenvalues are in general complex and finite, with $|z_m| < 1$. Each eigenvalue describes the exponential stroboscopic decay of the associated quasibound state—if the initial state is $|\psi_0\rangle = |\phi_m\rangle$, the intensity within the system decays as

$$\langle\psi_n|\psi_n\rangle = |z_m|^{2n}\langle\psi_0|\psi_0\rangle. \tag{3.21}$$

Writing $z_m = \exp[-i(\varepsilon_m - i\gamma_m/2)]$, the decay constant over a period T_0 is given by γ_m. As indicated, this decay constant is best viewed as arising from the imaginary part of a complex quasienergy $\varepsilon_m^\star = \varepsilon_m - i\gamma_m/2$, where the real part is defined modulo 2π.

Stroboscopic scattering with ideal contacts. We now turn the stroboscopic decay problem into a stroboscopic scattering problem. This requires to define how the escape from the system translates into particles detected outside, as well as how to feed particles into the system. In other words, we need to define objects that connect the state within the system (residing in the internal Hilbert space in which F and $\mathcal{Q}$ operate) to the amplitudes of the N incoming modes (states $|\psi_n^{(\mathrm{in})}\rangle$) and the N outgoing modes (states $|\psi_n^{(\mathrm{out})}\rangle$) outside the system.

In the case of ballistic coupling that we study thus far, the outgoing state can be taken of the simple form

$$|\psi_n^{(\mathrm{out})}\rangle = P|\psi_n\rangle, \tag{3.22}$$

with P such that $\mathcal{P} = P^T P = 1 - \mathcal{Q}$ recovers the rank-N projector that complements $\mathcal{Q}$ in the internal Hilbert space. It follows that $PP^T = 1$ is the identity in the space of the external scattering channels (the rank does not change under the reordering and the resulting object is still a projector). Recall that the internal state refers to the instance just before we open the system. Therefore, the incoming particle injected in the previous step modifies this state according to

$$\begin{aligned} |\psi_n\rangle &= F\mathcal{Q}|\psi_{n-1}\rangle + FP^T|\psi_{n-1}^{(\mathrm{in})}\rangle \\ &= (F\mathcal{Q})^n|\psi_0\rangle + \sum_{l=0}^{n-1}(F\mathcal{Q})^l FP^T|\psi_{n-l-1}^{(\mathrm{in})}\rangle, \end{aligned} \tag{3.23}$$

which replaces Eq. (3.19). Combining these expressions, we find

$$|\psi_n^{(\mathrm{out})}\rangle = P(F\mathcal{Q})^n|\psi_0\rangle + P\sum_{l=0}^{n-1}(F\mathcal{Q})^l FP^T|\psi_{n-l-1}^{(\mathrm{in})}\rangle. \tag{3.24}$$

The first part recovers the decay of the initial state, while the remaining part describes the scattering. The pure decay problem is characterised by the absence of the incoming state, while the pure scattering problem is characterised by the absence of the initial state.

Both these problems now turn out to be intimately related. For this, we revert back to a continuous time variable, $|\psi^{(\mathrm{out})}(t)\rangle = \sum_n \delta(t - nT_0)|\psi_n^{(\mathrm{out})}\rangle$, and perform a Fourier decomposition of the scattered signal,

$$|\psi^{(\mathrm{out})}(\varepsilon)\rangle = \sum_{n=0}^{\infty} e^{i\varepsilon n}|\psi_n^{(\mathrm{out})}\rangle \tag{3.25}$$

$$= \sum_{l=0}^{\infty}\sum_{n=l+1}^{\infty} e^{i\varepsilon l}P(F\mathcal{Q})^l e^{i\varepsilon}FP^T e^{i\varepsilon(n-l-1)}|\psi_{n-l-1}^{(\mathrm{in})}\rangle, \tag{3.26}$$

hence

$$|\psi^{(\mathrm{out})}(\varepsilon)\rangle = S(\varepsilon)|\psi^{(\mathrm{in})}(\varepsilon)\rangle \tag{3.27}$$

with the stroboscopic scattering matrix

$$S(\varepsilon) = P\sum_{l=0}^{\infty}[e^{i\varepsilon}F\mathcal{Q}]^l e^{i\varepsilon}FP^T = P\frac{1}{1 - e^{i\varepsilon}F\mathcal{Q}}e^{i\varepsilon}FP^T. \tag{3.28}$$

We now observe that the poles of the scattering matrix coincide with the complex quasienergies $\varepsilon_m^\star$, as determined by the eigenvalue problem (3.20).

It is convenient to bring the scattering matrix (3.28) into the equivalent form

$$S(\varepsilon) = \frac{P\mathcal{A}P^T - 1}{P\mathcal{A}P^T + 1}, \quad \mathcal{A} = \frac{1 + e^{i\varepsilon}F}{1 - e^{i\varepsilon}F} = -\mathcal{A}^\dagger. \tag{3.29}$$

We then see that the scattering matrix is indeed unitary. Furthermore, this expression nicely generalises to the case of non-ideal contacts, which we address next.

Stroboscopic scattering with non-ideal contacts. To account for non-ideal coupling we insert an energy-independent scatterer at the place of the contact. The contact can be viewed as a region with N channels coupled to the outside and N channels coupled to the inside, and thus is described by a $2N \times 2N$-dimensional unitary scattering matrix

$$S_B = \begin{pmatrix} r_B & t'_B \\ t_B & r'_B \end{pmatrix}. \tag{3.30}$$

The blocks r_B and r'_B describe the partial reflection in the external and internal channels, while t_B and t'_B describe the transmission into and out of the system. This matrix is assumed to be energy-independent, meaning that the reflection and transmission processes from the contact are instantaneous. The return of the particle to the contact is described by the ballistic scattering matrix S_0.

We can now match the waves at the contact according to Eq. (3.11), which results in the total scattering matrix

$$S = r_B + t'_B S_0 (1 - r'_B S_0)^{-1} t_B. \tag{3.31}$$

This expression has a simple interpretation: The incident wave is either directly reflected according to r_B, or enters into the system according to t_B. Once in the system, the wave undergoes a sequence of l events, each consisting of an internal scattering round trip S_0 followed by a partial reflection r'_B, until after another return S_0 to the contact it escapes according to t'_B. Equation (3.31) follows by summing over l, which is of the form of a geometric series.

Inserting for S_0 the stroboscopic scattering matrix (3.28) for ideal contacts, we find that this can be written more directly as

$$S = r_B + t'_B P \frac{1}{1 - e^{i\varepsilon}F(\mathcal{Q} + P^T r'_B P)} e^{i\varepsilon} F P^T t_B. \tag{3.32}$$

To further simplify this expression we choose an appropriate basis for the internal state, as well as for the incoming and the outgoing state. This follows from the polar decomposition (3.6), which we need to adopt in the slightly more general form

$$S_B = \begin{pmatrix} V & 0 \\ 0 & V' \end{pmatrix} \begin{pmatrix} -\Sigma\sqrt{1-\Gamma^2} & \sqrt{\Gamma} \\ \sqrt{\Gamma} & \Sigma\sqrt{1-\Gamma^2} \end{pmatrix} \begin{pmatrix} V'' & 0 \\ 0 & V''' \end{pmatrix}, \quad \begin{cases} \Gamma = \operatorname{diag}(\Gamma_n) \\ \Sigma = \operatorname{diag}(\sigma_n) \end{cases}. \tag{3.33}$$

Here $\Gamma_n \in [0, 1]$ are the transmission eigenvalues of the contact, while $\sigma_n = \pm 1$ discriminates two distinct ways to close a channel. The unitary matrices V, V', V'' and V''' can all be absorbed into the basis choice, which means that S_B is block diagonal

and real. Starting from (3.32), this basis choice results in the desired generalization of Eq. (3.29),

$$S = \frac{K\mathcal{A}K^T - 1}{K\mathcal{A}K^T + 1}, \quad \mathcal{A} = \frac{1 + e^{i\varepsilon}F}{1 - e^{i\varepsilon}F} = -\mathcal{A}^\dagger, \quad K = \mathrm{diag}\,(\kappa_n^{\sigma_n})P, \tag{3.34}$$

where the contact is now characterized by the coupling coefficients

$$\kappa_n = \Gamma_n^{-1/2}(1 - \sqrt{1 - \Gamma_n^2}). \tag{3.35}$$

These coefficients take the value $\kappa_n = 1$ for $\Gamma_n = 1$ and $\kappa_n \approx \sqrt{\Gamma_n}/2$ for $\Gamma_n \ll 1$. As they enter the matrix K to the power σ_n, a semitransparent contact can be achieved both by decreasing the coupling ($\sigma_n = 1$) or by increasing the coupling ($\sigma_n = -1$). This completes the derivation of the stroboscopic scattering matrix (3.18).

3.4.2 Continuous-time scattering theory

To realize the time-continuous limit of the stroboscopic scattering theory, we set $\varepsilon = ET_0/\hbar$, $F = \exp(-iT_0H/\hbar)$, and equate $T_0 \equiv 2\pi\hbar/M\Delta = T_H/M$ to the dwell time in a continuous system with M channels and mean level spacing Δ (this is the mean time for a round trip F in the system). In the leading orders of T_0, we can approximate

$$e^{i\varepsilon}F \approx \frac{1 - iT_0(H - E)/2\hbar}{1 + iT_0(H - E)/2\hbar}, \tag{3.36}$$

so that

$$\mathcal{A} = \frac{1 + e^{i\varepsilon}F}{1 - e^{i\varepsilon}F} \approx \frac{2i\hbar}{T_0}G(E), \quad G(E) = \frac{1}{E - H}, \tag{3.37}$$

where $G(E)$ is the Green function (or resolvent) of the closed system. For the ideal case with scattering matrix (3.29), we then have

$$S = \frac{\frac{2i\hbar}{T_0}P(E - H)^{-1}P^T - 1}{\frac{2i\hbar}{T_0}P(E - H)^{-1}P^T + 1}, \tag{3.38}$$

while for non-ideal leads P is replaced by K. Inserting T_0 completes the derivation of the Mahaux-Weidenmüller formula (3.17),

$$S(E) = \frac{i\pi W^\dagger(E - H)^{-1}W - 1}{i\pi W^\dagger(E - H)^{-1}W + 1}, \quad W = \frac{\sqrt{M\Delta}}{\pi}K^\dagger, \tag{3.39}$$

where the $M \times M$-dimensional hermitian matrix H represents the Hamiltonian of the closed systems, while the $M \times N$-dimensional matrix W describes the coupling to the N scattering channels. With our basis choice, W is diagonal, with elements

$$W_{nn} = \frac{\sqrt{M\Delta}}{\pi}\kappa_n^{\sigma_n} \tag{3.40}$$

specified according to Eq. (3.35). The form of W in the non-ideal case can also be obtained by starting with the scattering matrix (3.38) for ideal contacts and adding barriers by the construction (3.31).

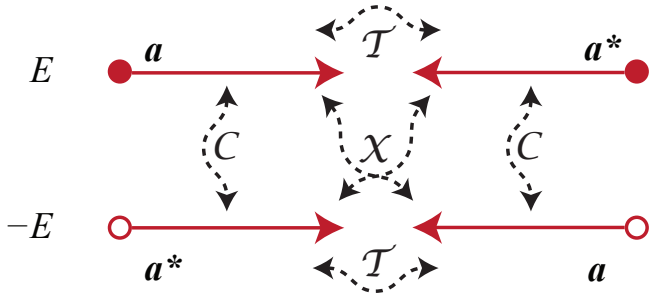

Fig. 3.3 Fundamental symmetries relate various states of motion, which constrains the scattering matrix in accordance to the ten universality classes for unitary matrix.

Equation (3.39) can be rewritten in the equivalent form

$$S(E) = -1 + 2\pi i W^\dagger (E - H + i\pi W W^\dagger)^{-1} W. \tag{3.41}$$

According to this, the poles of the scattering matrix are given by the eigenvalues of the effective non-hermitian Hamiltonian $H - i\pi W W^\dagger$. The poles all lie in the lower half of the complex plane, as required by causality. Furthermore, the Wigner-Smith time-delay matrix $Q = -i\hbar S^\dagger dS/dE$ takes the form

$$Q = 2\pi\hbar W^\dagger (E - H - i\pi W W^\dagger)^{-1} (E - H + i\pi W W^\dagger)^{-1} W, \tag{3.42}$$

which is explicitly positive semidefinite, as again required by causality.

3.5 Merits

Via the stroboscopic model (3.34), the orthogonal, unitary, or symplectic symmetry of F in the three Wigner-Dyson classes with different form of time-reversal symmetry translates directly into a corresponding symmetry of S. Via the continuous model (3.41), one finds that this also agrees with the corresponding symmetry class for H. In the symmetry classes with chiral or charge-conjugation symmetry, this translation holds when the scattering matrix is evaluated at the spectral symmetry points $E = 0$ or $\varepsilon = 0, \pi$ (away from these points, the symmetry reduces to the three Wigner-Dyson classes). Thus, the ten symmetry classes listed in Table 2.2 directly apply to the scattering matrix, with energy fixed to the symmetry point where required (Beenakker, 2015).

It is instructive to verify these statements directly within the scattering picture (see Fig. 3.3). For this, consider that the time-reversal operation $\mathcal{T}$ transforms incoming modes into outgoing modes. If this is a symmetry of the Hamiltonian then the correspondingly transformed scattering state must be described by the original scattering matrix. For $\mathcal{T} = K$ this delivers

$$\mathbf{a}^{(\mathrm{in})^*} = S(E)\mathbf{a}^{(\mathrm{out})^*} = S(E)S^*(E)\mathbf{a}^{(\mathrm{in})^*}, \tag{3.43}$$

such that $S^T(E) = S(E)$, as anticipated. Analogously, a time-reversal symmetry with $T = \Omega K$ implies $S^T(E) = \Omega S(E)\Omega^{-1}$, hence $[\Omega S(E)]^T = -\Omega S(E)$. For a

chiral symmetry $\mathcal{X}$, we transform a solution at energy E into a solution at energy $-E$. This inverts the group velocity of the propagating modes, thus again transforms incoming modes into outgoing modes. It follows that $\mathcal{X}S(E)\mathcal{X} = S^\dagger(-E)$, and hence $[\mathcal{X}S(-E)]^\dagger = \mathcal{X}S(E)$. For a charge-conjugation symmetry $\mathcal{C}$, both effects on the propagation direction cancel such that $S(-E) = S^*(E)$ if $\mathcal{C} = K$, while $S(-E) = \Omega S^*(E)\Omega^{-1}$ if $\mathcal{C} = \Omega K$. This recovers all constraints in Table 2.2.

Based on this correspondence, the effective scattering models deliver an independent view on the topological quantum numbers associated with the Hamiltonian (Fulga *et al.*, 2011; Beenakker, 2015; Schomerus *et al.*, 2015). In systems with a chiral symmetry, the matrix $S_{X0} = \mathcal{X}S(0)$ is unitary and hermitian, so that the trace $\nu_0 = \frac{1}{2}\mathrm{tr}\, S_X$ quantifies the difference between eigenvalues ± 1. According to Eq. (3.41) with a chiral Hamiltonian of the form (2.4), this topological quantum number can then be expressed as $\nu_0 = [\nu + (N_A - N_B)/2]_{|\nu_0| \leq N/2}$, where N_A and N_B count the number of channels coupled to the two different chiral sectors; as indicated by the brackets this saturates at $|\nu_0| = N/2$ where $N = N_A + N_B$. In systems with a charge-conjugation symmetry, where the Hamiltonian can be made anti-symmetric by an appropriate basis choice and displays a zero mode if M is odd (modulo possible Kramers degeneracy), $\nu_0 = \det S(0) = \nu$ (class D) and $\nu_0 = \mathrm{pf}\, \Omega S(0) = \nu$ (class DIII) remain directly related to the internal topological quantum number.

Beyond the pure symmetry classification, and perhaps even more importantly, the effective scattering models also determine the appropriate statistical ensembles for the scattering matrix for ergodic internal wave propagation (Brouwer, 1995). For ideal contacts, the circular ensembles for F translate via Eq. (3.28) into the corresponding circular ensembles for the ballistic scattering matrix S, with energy again fixed to the symmetry point where required. In the presence of a tunnel barrier, the Haar measure is deformed according to Eq. (3.34). In the three Wigner-Dyson classes this takes the form of a Poisson-kernel

$$P(S) \propto |\det(1 - \overline{S}^\dagger S)|^{-\beta N - 2 + \beta}, \tag{3.44}$$

where the non-ideal contacts are encoded in the average scattering matrix $\overline{S} = (1 - KK^T)/(1+KK^T)$. In the additional symmetry classes with chiral or charge-conjugation symmetry, the analogue of the Poisson kernel can be constructed based on Eq. (3.31) (Béri, 2009; Marciani *et al.*, 2016), which we briefly illustrate in Section 4.3.

By carrying out the continuum limit for large M, one furthermore finds that the internal Hamiltonian H in the Mahaux-Weidenmüller formula (3.39) complies with the corresponding Gaussian ensemble (see again Brouwer 1995). In the three Wigner-Dyson ensembles, the Cayley transform (3.36) implies at $E = 0$

$$F^\dagger dF = -i\Sigma dH \Sigma^\dagger, \quad \Sigma = \frac{1}{1 + iHT_0/2\hbar}, \tag{3.45}$$

which allows to calculate the Jacobian for the transformation from F to H. This leads to a Cauchy distribution

$$P(H) \propto \det(1 + H^2 T_0^2/4\hbar^2)^{-(\beta M + 2 - \beta)/2}, \tag{3.46}$$

which for large M shares all leading p-point correlations functions with the corresponding Gaussian ensemble.

These considerations provide a solid link between the random-matrix models for closed and open systems with ergodic internal dynamics. For ideal leads, the stationary scattering at fixed energy is described by a unitary scattering matrix from a circular ensemble, while the related Poisson kernel applies when the contacts are non-ideal. Based on the appropriate Gaussian ensemble for H, the effective scattering model can also be employed to study the energy-dependence, including the crossover between symmetry classes as the energy is steered away from a spectral symmetry point. Guided by the list of questions posed at the beginning of this chapter, we can now set out to describe scattering and decay from a random-matrix perspective.

4
Decay, Dynamics and Transport

We now turn to the random-matrix description of the physical phenomena outlined in Section 3.3.

4.1 Scattering poles

According to the Mahaux-Weidenmüller formula (3.41), the complex energies of the quasibound states (poles of the scattering matrix) are obtained from the eigenvalue problem

$$E_m|\phi_m\rangle = H_{\text{eff}}|\phi_m\rangle, \tag{4.1}$$

where the $M \times M$ dimensional effective non-hermitian Hamiltonian is of the form $H_{\text{eff}} = H - i\pi WW^\dagger$ (Fyodorov and Sommers, 1997; Fyodorov and Sommers, 2003; Fyodorov and Savin, 2011). This consists of a hermitian part H which represents the dynamics in the closed system, and an anti-hermitian part involving a positive semidefinite matrix $WW^\dagger$ of rank N. The eigenvalues are therefore confined to the lower half of the complex plane, where $\operatorname{Im} E_m = -\hbar\gamma_m/2$ encodes the positive decay rates γ_m. Analogously, the poles of the stroboscopic scattering matrix can be read off Eq. (3.32), according to which they are obtained from the eigenvalue problem

$$z_m|\phi_m\rangle = F(\mathcal{Q} + P^T r'_B P)|\phi_m\rangle, \tag{4.2}$$

with $z_m = \exp(-i\varepsilon_m)$ confined by $|z_m| \leq 1$. The two problems are then related by identifying $\varepsilon_m = E_m T_0/\hbar$ with $T_0 = 2\pi\hbar/M\Delta$; see our discussion in Section 3.4.2.

In a random-matrix description with large matrix dimension M, one typically finds that the eigenvalues populate a well-defined region, with universal statistics in the bulk (Fyodorov and Khoruzhenko, 1999; Forrester, 2010; Khoruzhenko and Sommers, 2011). In particular, well inside the eigenvalue support the level repulsion is typically captured by a factor $\prod_{n<m} |E_n - E_m|^2$, as already encountered for the Ginibre ensembles, which then yields cubic level repulsion. For many physical applications, however, we are mainly interested in the properties of the longest-living modes in a given energy range, which approach the real axis closest from below, and are automatically situated at the boundary of the spectral support. These modes determine the noticeable resonance patterns that one observes, e.g., in the scattering and decay of nuclei (Weidenmüller and Mitchell, 2009) or in the emission properties of optical microresonators (Cao and Wiersig, 2015). To determine their properties we need to work directly with the effective scattering models.

Particularly compact expression for the distribution of decay rates can be obtained for the stroboscopic model (3.28) with ideal leads (Zyczkowski and Sommers, 2000).

The quasi-bound states are then obtained from the eigenvalue problem (3.20) for the truncated time-evolution operator $F\mathcal{Q}$. We assume that $F \in \mathrm{U}(M)$ is a random unitary matrix of dimension $M \times M$, distributed according to the Haar measure $\mu(F)$, which places us into the circular unitary ensemble (CUE) for systems without any further symmetries. Averaging over this ensemble, it is then possible to determine the density of eigenvalues z_m in the complex plane. In a first step, one finds the joint distribution of the nontrivial eigenvalues $z_m \neq 0$, to which we assign the indices $m = 1, 2, \ldots, M-N$. This joint distribution is given by

$$P(\{z_m\}) \propto \prod_{i<j}^{M-N} |z_i - z_j|^2 \prod_{k=1}^{M-N} (1 - |z_k|^2)^{N-1}, \tag{4.3}$$

where the first term signifies the expected level repulsion. The density of the eigenvalues in the complex plane follows by integrating out all but one eigenvalue, which gives

$$\rho(z) \propto (1 - |z|^2)^{N-1} \sum_{l=1}^{M-N} \frac{(N+l-1)!}{(l-1)!} |z|^{2l-2} \quad \text{for } |z| < 1. \tag{4.4}$$

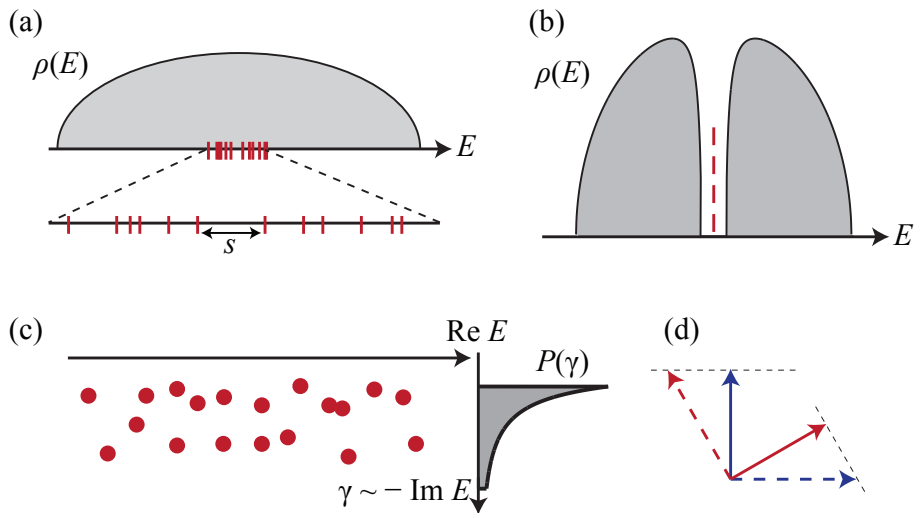

Fig. 4.1 (a) In a closed system, energy levels are constrained to be real, and random-matrix theory focusses on the spectral fluctuations, e.g. of the level spacings s. These occur against the non-universal backdrop of the mean density of states $\rho(E)$, here illustrated as the Wigner semicircle law (2.3). (b) Fundamental symmetries can introduce spectral symmetries which induce universal aspects into the mean density of states. At the symmetry point, topologically protected zero modes can appear. This is here illustrated for the case of the chiral symmetry, with the mean density of states given by Eq. (2.7). (c) In an open system, the corresponding energies are complex and attention shifts to the decay rates γ of the states, here given in accordance to Eq. (4.10). (d) The states become non-orthogonal, which requires to introduce a bi-orthogonal system as here illustrated for a pair of states.

This density has several interesting limits. For $M, N \to \infty$ at fixed $N/M = 1 - \mu$, the modulus $r = |z|$ obeys

$$P(r) = (\mu^{-1} - 1)\frac{2r}{(1-r^2)^2}\Theta(\mu - r^2), \tag{4.5}$$

while for $M \to \infty$ at fixed N we have, setting $(1-r)/T_0 \to \gamma/2$,

$$P(\gamma) = \frac{\gamma^{N-1}}{(N-1)!}\left(\frac{-d}{d\gamma}\right)^N \frac{1 - e^{-\gamma T_H}}{\gamma T_H}, \tag{4.6}$$

where $T_H = 2\pi\hbar/\Delta$ is the Heisenberg time.

According to Eq. (4.5), in the considered limit all poles are confined to the region $r < \sqrt{\mu}$, thus do not approach the unit circle closely. Such a hard gap is also obtained from large-N limit of equation (4.6) (thus $1 \ll N \ll M$), in which

$$P(\gamma) = \frac{\gamma_0}{\gamma^2} \quad \text{if } \gamma > \gamma_0, \quad 0 \text{ otherwise.} \tag{4.7}$$

Here $\gamma_0 = N\Delta/2\pi\hbar = 1/T_D$ coincides with the classical decay rate out of a system with dwell time $T_D = T_H/N$. The corresponding energy scale $E_{\rm Th} = \hbar/T_D = N\Delta/2\pi$ is known as the Thouless energy.

These results recover the main features earlier obtained by a direct analysis of the non-hermitian eigenvalue problem (4.1). The most comprehensive insight is obtained using supersymmetric integration techniques, which predict Eq. (4.6) for ideal coupling and extend it to non-ideal leads (Fyodorov and Sommers, 1996; Fyodorov and Sommers, 1997; Fyodorov and Sommers, 2003). The result is

$$\begin{aligned} P(\gamma) &= \frac{\hbar\pi}{\Delta}\mathcal{F}_1\left(\frac{\hbar\pi}{\Delta}\gamma\right)\mathcal{F}_2\left(\frac{\hbar\pi}{\Delta}\gamma\right), \\ \mathcal{F}_1(y) &= \frac{1}{2\pi}\int_{-\infty}^{\infty} dx\, e^{-ixy}\prod_{n=1}^{N}\frac{1}{x_n - ix}, \quad \mathcal{F}_2(y) = \frac{1}{2}\int_{-1}^{1} dx\, e^{-xy}\prod_{n=1}^{N}(x_n + x), \end{aligned} \tag{4.8}$$

where $x_n = -1 + 2/\Gamma_n$ encodes the transparency of the contact. For a barrier with uniform transparency Γ (hence dimensionless conductance $g_c = \Gamma N$), the distribution function can be written compactly as

$$P(\gamma) = \frac{\Delta}{2\pi\hbar\gamma^2(N-1)!}\int_{N(1-\Gamma)\gamma/\gamma_0}^{N\gamma/\gamma_0} dx\, x^N e^{-x}, \tag{4.9}$$

where now $\gamma_0 = \Gamma N\Delta/2\pi\hbar$. The large-$N$ limit (4.7) is then replaced by

$$P(\gamma) = \frac{\gamma_0}{\Gamma\gamma^2} \quad \text{if } \gamma_0 < \gamma < \gamma_0/(1-\Gamma), \tag{4.10}$$

so that the decay rates are reduced according to the increased classical dwell time $T_D = T_H/(\Gamma N)$.

The random-matrix results for the unitary symmetry class can be extended to the other symmetry classes. As with the Ginibre ensembles, many of the common characteristics remain unchanged, with the main modifications arising from spectral symmetries. In particular, in systems with time-reversal symmetry (orthogonal and symplectic symmetry class) no further spectral symmetries arise (these cases are therefore quite distinct from the real and symplectic Ginibre ensemble, which lends further justification to their careful construction). The main modifications arise from the altered level repulsion in the closed limit, which is felt by the longest-living states (Sommers *et al.*, 1999; Fyodorov and Savin, 2011). At large matrix dimensions N and M, these modifications do not matter and a hard gap of order γ_0 again emerges for the decay rates (Haake *et al.*, 1992; Lehmann *et al.*, 1995; Janik *et al.*, 1997). This induces the emergence of classical exponential decay in the time domain (Savin and Sokolov, 1997).

In the classes with chiral or charge-conjugation symmetries, all poles come in pairs E_l, $-E_l^*$ which are symmetrically arranged with respect to the imaginary axis $\operatorname{Re} E = 0$. The exception are unpaired modes pinned to the imaginary axis, $\operatorname{Re} E_l = 0$, that arise from the zero modes in the closed setting, and add a topological feature to the complex spectrum (Pikulin and Nazarov, 2012; Pikulin and Nazarov, 2013). These symmetry-respecting poles can only depart from the imaginary axis in pairs, involving an exceptional point where two poles meet as described in Section 2.5. Thus, for an odd number of zero modes at least one such pole is always confined to the imaginary axis. For a superconducting system these poles describe Majorana zero modes that seep out of the system (Pikulin and Nazarov, 2012; Pikulin and Nazarov, 2013; San-Jose *et al.*, 2016), while in a photonic setting they can be employed for selective amplification (Schomerus and Halpern, 2013; Schomerus, 2013*b*; Poli *et al.*, 2015). Within random-matrix theory, we describe the consequences for the density of states in Section 4.3.

In the construction of the effective scattering models we noted that channels can also be closed by increasing the coupling beyond a certain threshold ($\sigma_n = -1$ in Eq. (3.34) or Eq. (3.40)). Physically this should again result in a reduced decay rate γ_0 of the longest-living modes. The spectral decomposition of the effective Hamiltonian, on the other hand, implies the sum rule

$$\operatorname{Im} \operatorname{tr} (H - i\pi W W^\dagger) = -\pi \operatorname{tr} W W^\dagger = \sum_m \operatorname{Im} E_m, \tag{4.11}$$

so that the sum of all decay rates must grow. These two expectations can be reconciled in a careful analysis which shows that N' strongly coupled channels result in a corresponding number of poles with very short life time (Haake *et al.*, 1992). These poles are then well-separated from the poles describing the long-living states, which retain a typical decay rate $\gamma_0 = \Gamma N \Delta / 2\pi\hbar$. This nontrivial reorganisation of the complex spectrum is known as resonance trapping (Rotter, 2009). In the symmetry classes with charge-conjugation symmetry, it can affect the Majorana pole pinned to the imaginary axis, which justifies to identify the case of ideal coupling as a topological phase transition (Akhmerov *et al.*, 2011; Marciani *et al.*, 2016).

The appearance of the classical decay rate in these considerations indicates that random-matrix theory is only applicable if the system-specific details become indis-

cernible before the classical dwell time $T_D = T_H/(\Gamma N)$. For a contact with dimensionless conductance $g_c = \Gamma N \gg 1$, this condition is more stringent than the requirement in the closed system, where T_D is replaced by T_H. A common occurrence where this condition is mildly violated are systems with ballistic decay routes, which result in additional short-living states that often form interweaving bands deep in the complex plane (Weich *et al.*, 2014). In a classically chaotic systems, these routes apply to trajectories that escape before the Ehrenfest time $T_{\rm Ehr} \approx \lambda^{-1} \ln N$, where λ is the Lyapunov exponent (Berman and Zaslavsky, 1978; Aleiner and Larkin, 1996; Schomerus and Jacquod, 2005). In the limit of large N and M, the fraction of long-living modes is then reduced by a factor $\exp(-T_{\rm Ehr}/T_D) = N^{-1/(\lambda T_D)}$ (Schomerus and Tworzydło, 2004), a power-law which agrees with a picture where these states are confined to the classical repeller (Lu *et al.*, 2003; Keating *et al.*, 2006). This modification due to ballistic chaotic decay is known as the fractal Weyl law (Nonnenmacher and Zworski, 2005). In practice, random-matrix theory still provides a good description of the remaining long-living modes (Schomerus *et al.*, 2009). Furthermore, partial reflections at the contacts and disorder are very effective mechanisms to remove the ballistic decay routes.

4.2 Mode non-orthogonality

Since the effective Hamiltonian $H_{\rm eff} = H - i\pi WW^\dagger$ is non-hermitian, the quasibound states $|\phi_m\rangle$ from the eigenvalue problem (4.1) do not form an orthonormal basis. In a given basis, we thus have a spectral decompositions $H_{\rm eff} = VDV^{-1}$, $D = {\rm diag}\,(E_m)$ where the matrix V is not unitary. The extent of mode non-orthogonality is then quantified by the condition numbers O_{mn} introduced in Eq. (2.20).

In order to get insight into the significance of these objects we consider the divergent part

$$\mathrm{tr}\, S^\dagger S \approx \mathrm{tr} 2\pi W^\dagger (E - H - i\pi WW^\dagger)^{-1} 2\pi W^\dagger W (E - H + i\pi WW^\dagger)^{-1} W \equiv \sigma(E) \quad (4.12)$$

of the scattering strength for a complex energy close to a pole, $E \to E_n$ (Schomerus *et al.*, 2000). Using the spectral decomposition for the effective Hamiltonian we find

$$\sigma(E) = \sum_{nm} \frac{-(E_n - E_m^*)^2}{(E - E_n)(E - E_m^*)} O_{mn}, \quad (4.13)$$

where we used $2\pi WW^\dagger = iH_{\rm eff} - iH_{\rm eff}^\dagger = iVDV^{-1} - iV^{-1\dagger} D^* V^\dagger$. Very close to the pole, $\sigma(E) \approx \frac{(\hbar\gamma_n)^2}{|E-E_n|^2} K_n$ describes a Breit-Wigner resonance with peak height proportional to $K_n = O_{nn}$. Thus, the factors K_n are directly related to the scattering strengths of the quasibound states.

Energies in the complex plane are effectively probed in amplifying photonic systems, which can be described in a scattering approach that is amended to account for radiation created within the medium (Beenakker, 1998; Schomerus *et al.*, 2000; Schomerus, 2009). Under ideal conditions, an active medium with amplification rate γ_a can generate spontaneously amplified radiation with frequency-resolved intensity

$$I(\omega) \approx (2\pi)^{-1}\, \mathrm{tr}\, (S^\dagger S - 1)|_{E = \hbar\omega - i\hbar\gamma_a/2}. \quad (4.14)$$

Close to the laser threshold, a single pole $E_m = \hbar\omega_m$ lies close to the real axis, producing a well-isolated Lorentzian emission line

$$I(\omega) \approx \frac{K_m}{2\pi} \frac{\gamma_n^2}{(\omega - \omega_m)^2 + (\gamma_m - \gamma_a)^2/4}. \tag{4.15}$$

In this context, K_m is know as the Petermann factor and signifies excess noise (Petermann, 1979).

For lasers we can ignore magneto-optical effects, and thus are concerned with the orthogonal symmetry class where the effective Hamiltonian inherits the symmetry $H_{\rm eff} = H_{\rm eff}^T$. In this case we can normalise the right and left eigenstates so that $V^{-1} = V^T$ and find

$$K_m = |(V^\dagger V)_{mm}|^2. \tag{4.16}$$

As described in Section 2.5 for the Ginibre ensemble, the Petermann factor of modes in the bulk of the complex spectrum should be large. For the effective Hamiltonian $H_{\rm eff}$ with $N, M \gg 1$, this can be verified in the free-probability approach (Janik *et al.*, 1997), according to which

$$\overline{K_m}\,|_{\gamma_m=\gamma} \approx N \left(\frac{\gamma}{\gamma_0} - 1\right) \left(1 - \frac{(1-\Gamma)\gamma}{\gamma_0}\right) \tag{4.17}$$

for decay rates well within the range $\gamma_0 < \gamma < \gamma_0/(1-\Gamma)$. However, this result breaks down close to the edges of the spectrum, where it violates the constraint $K_m \geq 1$, and hence does not apply to the long-living states that become the lasing modes.

These restrictions can be circumvented by the same supersymmetric techniques that address the poles (Schomerus *et al.*, 2000). Equation (4.8) is then supplemented by

$$\overline{K_m}\,|_{\gamma_m=\gamma} = 1 + \frac{2\pi\hbar}{\Delta} \frac{S(\pi\hbar\gamma/\Delta)}{P(\gamma)}, \quad S(y) = -\int_0^y dy'\, \mathcal{F}_1(y') \frac{\partial}{\partial y'} \mathcal{F}_2(y'), \tag{4.18}$$

which for identical transparencies $\Gamma_n = \Gamma$ can be brought into a compact form using

$$S(\pi\gamma/\hbar\Delta) = \frac{\Delta^2}{(2\pi\hbar\gamma)^2 (N-1)!} \int_{N(1-\Gamma)\gamma/\gamma_0}^{N\gamma/\gamma_0} dx\, x^{N-1} e^{-x} \left(\frac{N(1-\Gamma)\gamma}{\gamma_0} - x\right) \left(x - \frac{N\gamma}{\gamma_0}\right). \tag{4.19}$$

For large N, where we can apply a saddle-point approximation, it follows that the Petermann factor $\overline{K_m}\,|_{\gamma_m=\gamma_0} \sim \Gamma(\sqrt{2N/\pi} + 4\pi/3)$ of the long-living modes can still be parametrically large in N. When a large number L of such modes compete for the gain, the large-deviation tail of the decay-rate distribution (4.6) is probed, which reduces K_m by a factor $\sim 1/\sqrt{\ln L}$. For $\Gamma N \ll 1$, on the other hand, the system is almost closed, and $K_m \sim 1$ as mode-orthogonality is restored. Similarly, for $N = 1$ the typical Petermann factor $K_m \sim 1 + \Gamma\hbar\gamma_m/\Delta$ is also close to unity.

In all these cases, the Petermann factors of individual states can be much larger than the typical values quoted above. This is the case because K_m diverges if two complex eigenvalues become degenerate, thus, as one approaches an exceptional point.

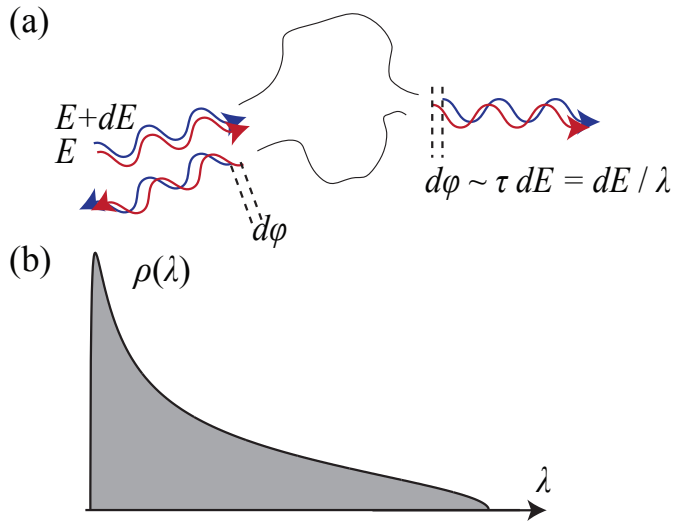

Fig. 4.2 (a) The Wigner-Smith delay times τ extract dynamical information by considering the energy sensitivity of the scattering phase in stationary scattering states. (b) Distribution of rates $\lambda = \tau^{-1}$ from random scattering, as predicted by the Marchenko-Pastur law (2.14) for the Wishart-Laguerre ensemble.

The cubic level repulsion makes such approaches rare, but long power tails still emerge in the probability distribution of K_m.

We mentioned that the Petermann factor signifies an enhanced sensitivity to noise generated by spontaneous emission. Similar considerations apply when external parameters are changed. A perturbative treatment then reveals an enhanced response compared to systems with orthogonal modes, which is again quantified by the mode non-orthogonal matrix (Fyodorov and Savin, 2012). Close to an exceptional point, where the eigenvectors become degenerate and K_m diverges, the significantly enhanced response can be exploited for sensors (Wiersig, 2014). This enhanced sensitivity also applies to the topological spectral transitions in non-hermitian systems with a chiral or charge-conjugation symmetry (where they occur on the imaginary axis), or non-hermitian systems with a parity-time symmetry (where they occur on the real axis). The radiation emitted from a parity-time symmetric photonic system indeed diverges when one closes the system (Schomerus, 2010). For an open system close to an exceptional point, on the other hand, the formal divergence of the Petermann factor signifies a change of the line shape from the Lorentzian (4.14) to a squared Lorentzian (Yoo *et al.*, 2011).

4.3 Delay times

We now turn to the Wigner-Smith time-delay matrix $Q = -i\hbar S^\dagger dS/dE$, which according to the Mahaux-Weidenmüller formula (3.41) can be written in the form (3.42),

$$Q = 2\pi\hbar W^\dagger (E - H - i\pi WW^\dagger)^{-1}(E - H + i\pi WW^\dagger)^{-1}W. \tag{4.20}$$

This matrix is manifestly hermitian and positive-definite, as required by causality. According to the Birman-Krein formula (3.10), the density of states is then given by

$$\rho(E) = \operatorname{tr} W^\dagger (E - H - i\pi W W^\dagger)^{-1} (E - H + i\pi W W^\dagger)^{-1} W, \tag{4.21}$$

which is of a similar form as the scattering strength $\sigma(E)$ in Eq. (4.12). Using the spectral decomposition for the effective Hamiltonian we find

$$\begin{aligned} \rho(E) &= \frac{1}{2\pi} \sum_{nm} i \frac{(E_n - E_m^*)}{(E - E_n)(E - E_m^*)} O_{mn} \\ &= -\frac{1}{\pi} \operatorname{Im} \sum_n \frac{1}{(E - E_n)}, \end{aligned} \tag{4.22}$$

where we used $\sum_n O_{nm} = \sum_m O_{nm} = 1$. Close to an isolated resonance $E \approx E_n$ this approaches $\rho(E) \approx \frac{1}{\pi} \frac{\operatorname{Im} E_n}{|E - E_n|^2}$, which is a Lorentzian normalised to 1.

More direct insight into this problem is obtained from the proper delay times τ_n, defined as the eigenvalues of Q, which are all real and nonnegative. We first consider the case of ballistic coupling. In the three standard classes (Brouwer *et al.*, 1997), it is useful to consider the matrix $Q_S = S^{1/2} Q S^{-1/2}$, which has the same eigenvalues but whose statistical distribution is the independent of S itself, so that $P(S, Q_S) = P(S)P(Q_S)$. Perturbation theory around the point where $S = -1$ then shows that the positive-definite rate matrix Q_S^{-1} follows the distribution

$$P(Q_S^{-1}) \propto (\det Q_S^{-1})^{N\beta/2} \exp[-(\beta T_H/2) \operatorname{tr} Q_S^{-1}], \tag{4.23}$$

with the Heisenberg time $T_H = 2\pi\hbar/\Delta$. This resembles a Wishart-Laguerre ensemble (2.12), but is directly expressed for Q_S and supplemented with a determinantal factor. The joint distribution of rates $\lambda_n = 1/\tau_n$ is given by

$$P(\{\lambda_n\}) \propto \prod_{n<m} |\lambda_n - \lambda_m|^\beta \prod_k \lambda_k^{N\beta/2} \exp(-\beta \lambda_k T_H/2), \tag{4.24}$$

which indeed looks formally identical to the eigenvalue distribution (2.13) of a Wishart matrix, albeit with half-integer dimensions if $\beta = 4$. This still constitutes a Wishart-Laguerre ensemble.

The same independence of S and Q_S also occurs in the four classes with charge-conjugation symmetry at the symmetry point $E = 0$ (Marciani *et al.*, 2014), where

$$P(\{\lambda_n\}) \propto \prod_{n<m} |\lambda_n - \lambda_m|^{\beta_T} \prod_k \lambda^{\beta_T' + N\beta_T/2} \exp(-\beta_T'' \lambda_k T_H/2) \tag{4.25}$$

with $\beta_T = 1, 2, 4, 2$, $\beta_T' = -1, -1, 2, 1$, $\beta_T'' = 1, 2, 2, 1$ in the symmetry classes D, DIII, C, CI. In the classes C and CI all delay times occur in degenerate pairs, which in Eq. (4.25) are only accounted for once.

In contrast, the chiral symmetry condition $S(E) = \mathcal{X} S^\dagger(-E) S^\dagger$ implies that the hermitian unitary matrix $S_{X0} = \mathcal{X} S(0)$ commutes with $Q(0)$, so that both matrices share a common structure (Schomerus *et al.*, 2015). Recall that S_{X0} has eigenvalues

± 1, whose frequency is captured by the topological quantum number $\nu_0 = \frac{1}{2}\mathrm{tr}\, S_{X0} = [\nu + (N_A - N_B)/2]_{|\nu_0|\leq N/2}$ (see Section 3.5). Correspondingly, the delay times can be grouped into two sets, made of $N_+ = N/2 + \nu_0$ delay times $\tau_n^+ = 1/\lambda_n^+$ associated with the subspace where the eigenvalues of S_{X0} are 1, and $N_- = N/2 - \nu_0$ delay times $\tau_n^- = 1/\lambda_n^-$ associated with the subspace where the eigenvalues of S_{X0} are -1. These two sectors can be made manifest by considering the reordered matrix

$$\tilde{Q}(E) = 2\pi\hbar(E - H + i\pi WW^\dagger)^{-1}WW^\dagger(E - H - i\pi WW^\dagger)^{-1}, \tag{4.26}$$

which has the same non-vanishing eigenvalues as Q. Inserting here the chiral Hamiltonian (2.4) and splitting the coupling matrix analogously into blocks $W = \mathrm{diag}\,(W_A, W_B)$ describing N_A and N_B open channels, respectively, this reordered matrix becomes block diagonal,

$$\tilde{Q}(0) = 2\pi\hbar\,\mathrm{diag}\,(\Lambda_-^{-1}, \Lambda_+^{-1}) \tag{4.27}$$

where

$$\Lambda_- = \pi^2 W_A W_A^\dagger + A(W_B W_B^\dagger + 0^+)^{-1}A^\dagger, \tag{4.28}$$

$$\Lambda_+ = \pi^2 W_B W_B^\dagger + A^\dagger(W_A W_A^\dagger + 0^+)^{-1}A. \tag{4.29}$$

In the subspaces where these two matrices are finite, we can write $\Lambda_\pm = X_\pm^\dagger X_\pm$ with an $N \times N_\pm$ dimensional matrix X. For large M, the matrix X tends to a random Gaussian matrix, so that the two sets of decay rates are both obtained from a Wishart-Laguerre ensemble,

$$P_\pm(\{\lambda_n^\pm\}) = \prod_{n<m} |\lambda_n^\pm - \lambda_m^\pm|^\beta \prod_k \lambda_k^{\beta/2-1+(\beta/4)|N\mp 2\nu\pm N_B\mp N_A|} e^{-\beta\lambda_k T_H/4}. \tag{4.30}$$

The two sets are independent of each other, whereby the full joint distribution factorises according to $P(\{\lambda_n^+, \lambda_n^-\}) = P_+(\{\lambda_n^+\})P_-(\{\lambda_n^-\})$.

We note that the joint distribution (4.25) does not involve the topological quantum number ν defined in classes D and DIII. In the chiral ensembles, on the other hand, the topological zero modes directly affect the joint distribution (4.30). This dependence also transfers to the mean density of states, which is given by

$$\overline{\rho} = \frac{1}{\Delta}\frac{N/2(N/2 + 1 - 2/\beta) + \nu_0^2}{(N/2 + 1 - 2/\beta)^2 - \nu_0^2} \quad \text{for } |\nu_0| < N/2, \tag{4.31}$$

$$\overline{\rho} = \frac{1}{\Delta}\frac{N/2}{|\nu - \nu_0 + (N_A - N_B)/2| + 1 - 2/\beta} \quad \text{for } |\nu_0| = N/2, \tag{4.32}$$

with the exceptions $|\nu - N_B| \leq 1$ or $|\nu + N_A| \leq 1$ (for $\beta = 1$) and $\nu = N_B$ or $\nu = -N_A$ (for $\beta = 2$) where the ensemble-average diverges.

These considerations can be extended to non-ideal leads (Marciani *et al.*, 2016), where one relates the scattering matrix S via Eq. (3.31) to the scattering matrix S_0 for ballistic coupling. The time-delay matrix then changes from Q_{S0} to $Q_S = \Sigma Q_{S0}\Sigma^\dagger$, where $\Sigma = (1 - S^\dagger r_B)^{-1}t_B$. The transformation of the probability measure follows

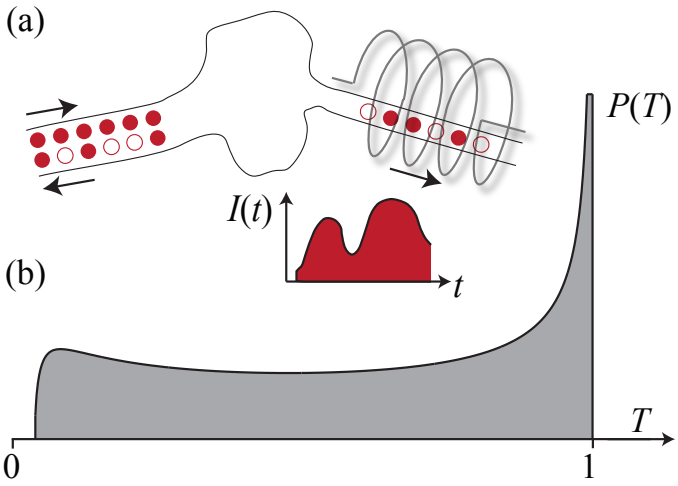

Fig. 4.3 (a) Phase-coherent electronic transport is characterised by partition noise, generated by the transmission of charge carriers with probability T. This noise can be detected in the current fluctuations $I(t)$. (b) Mean density of transmission probabilities T from Eq. (4.37), in accordance to the Jacobi ensemble of random-matrix theory.

from the analogous relation $S^\dagger dS = \Sigma(S_0^\dagger dS_0)\Sigma^\dagger$. For the standard symmetry classes, the factorised distribution $P(S_0, Q_{S0}^{-1}) = P(S_0)P(Q_{S0}^{-1})$ transforms into

$$P(S, Q_S^{-1}) = (\det \Sigma\Sigma^\dagger)^{N\beta/2}(\det Q_S^{-1})^{N\beta/2} \exp[-(\beta T_H/2)\,\mathrm{tr}\,\Sigma^\dagger Q_S^{-1}\Sigma], \tag{4.33}$$

while in the classes with charge-conjugation symmetry this takes the form

$$P(S, Q_S^{-1}) = (\det \Sigma\Sigma^\dagger)^{N\beta_T/2}(\det Q_S^{-1})^{N\beta_T/2+\beta'_T} \exp[-(\beta''_T T_H/2)\,\mathrm{tr}\,\Sigma^\dagger Q_S^{-1}\Sigma]. \tag{4.34}$$

The density of states $\rho = 2\pi\hbar^{-1}\,\mathrm{tr}\,\Sigma Q_{S0}\Sigma^\dagger$ can then be analysed directly using the independence of S (appearing in Σ) and Q_{S0}. By definition, $\mathrm{tr}\,\overline{Q_{S0}} = 2\pi\hbar\rho_0$ is given by the density of states for ideal coupling, while the scattering matrix itself follows the Poisson kernel distribution $P(S) \propto |\det(1 - r_B^\dagger S)|^{-\beta_T N - 2 + \beta_T - 2\beta'_T}$ (recovering the result of Béri 2009). In class D, a barrier with mode-independent transparency Γ then yields the mean density of states

$$\overline{\rho} = \frac{N}{(N-2)\Delta}\left(1 - \frac{2}{N\Gamma}[\Gamma - 1 + (-1)^\nu(1-\Gamma)^{N/2}]\right), \tag{4.35}$$

which now depends on ν. More generally, in classes D and DIII a topological zero mode remains visible as long as none of the couplings are fully ballistic.

4.4 Transport

Some of the best tested applications of random scattering matrices arise when one considers the low-temperature transport of electrons through a mesoscopic device in

response to a small bias voltage V_b. These applications have been covered in two comprehensive reviews considering the standard ensembles (Beenakker, 1997) and the additional ensembles with chiral or charge-conjugation symmetry (Beenakker, 2015), supplemented by a detailed review on shot noise (Blanter and Büttiker, 2000), and we refer to these sources throughout the section. In keeping with the rest of these notes we remain focussed on situations where the details of the geometry do not matter (this ignores the effects of Anderson localization, which we briefly pick up in the next Chapter 5). For the scattering at a fixed energy we are then directly led to the circular ensembles. This was first utilised by Blümel and Smilansky (1990), who found that the statistics of phase shifts from chaotic scattering agree with Eq. (2.11), while the applications to transport were pioneered by Baranger and Mello (1994) and Jalabert *et al.* (1994).

In the scattering approach to transport, the device is modelled as a scattering region attached to a left and a right lead, so that the scattering matrix is of the form (3.5). The quantities of interest are the transmission eigenvalues $T_n \in [0,1]$ of $t^\dagger t$, with the dimensionless conductance given by $g = \sum_n T_n$. We shall assume that the number of channels $N_R \geq N_L$ so as to avoid $N_L - N_R$ vanishing eigenvalues (otherwise we can simply study the eigenvalues of $tt^\dagger$). In the three standard circular ensembles (COE, CUE and CSE), the joint distribution of the transmission eigenvalues is then given by

$$P(\{T_n\}) \propto \sum_{n<m} |T_n - T_m|^\beta \prod_k T_k^{-1+\beta(1+|N_L-N_R|)/2}, \tag{4.36}$$

which can be interpreted as a Jacobi ensemble for variables $\mu_n = 1 - 2T_n$.

For large number of channels $N_L, N_R \gg 1$, the mean density of eigenvalues converges to

$$\rho(T) = \frac{N_L + N_R}{2\pi T} \left(\frac{T - T_c}{1 - T}\right)^{1/2} \tag{4.37}$$

for $1 > T > T_c = (N_L - N_R)^2/(N_L + N_R)^2$; for $N_L = N_R$ this takes the form

$$\rho(T) = \frac{N_L}{\pi} \frac{1}{\sqrt{T(1-T)}}. \tag{4.38}$$

In leading order of $N_L, N_R \gg 1$, Eq. (4.37) gives the ensemble-averaged dimensionless conductance $\overline{g} = N_L N_R/(N_L + N_R)$, so that $\overline{g}^{-1} = N_L^{-1} + N_R^{-1}$ resembles the series addition of two resistances. The exact result for finite N_L and N_R is

$$\overline{g} = \frac{N_L N_R}{N_L + N_R - 1 + 2/\beta}, \tag{4.39}$$

so that the next-to-leading reads

$$\overline{g} - \frac{N_L N_R}{N_L + N_R} \approx (1 - 2/\beta) \frac{N_L N_R}{(N_L + N_R)^2} \quad \text{for } N_L, N_R \gg 1. \tag{4.40}$$

This ensemble-dependent correction, known as weak localization (for $\beta = 1$) and as weak anti-localization (for $\beta = 4$), can be related to the factors $T_k^{-1+\beta/2(1+|N_L-N_R|)}$

in the joint distribution (4.36), which induce a bias of the transmission eigenvalues to small or large values. The joint distribution also determines the variance of the conductance within the ensemble,

$$\operatorname{var} g \approx \frac{(N_L N_R)^2}{\beta(N_L+N_R)^4} \quad \text{for } N_L, N_R \gg 1. \tag{4.41}$$

Due to the repulsion $\sim |T_n - T_m|^\beta$ of the eigenvalues this variance is small, but depends on the symmetry class already in leading non-vanishing order.

In a more general picture, the transmission eigenvalues determine the full counting statistics of the electrons that pass through the system. Let $Q(s)$ be the accumulated charge over a time interval s, via the arrival of electrons with elementary charge $\mathbf{e}$. In each eigenchannel, an incoming electron is transmitted with probability T_n, so that the counting statistics are given by a Bernoulli process. Noting that these transmission events occur with an attempt rate $\mathbf{e}V_b/h$ (with $h = 2\pi\hbar$), this process is described by the cumulant-generating function (Levitov and Lesovik, 1993)

$$\ln\langle \exp(pQ(s)/\mathbf{e})\rangle = \sum_{k=1}^{\infty} \langle\langle Q(s)\rangle\rangle \frac{p^k}{\mathbf{e}^k k!} = s(\mathbf{e}V_b/h) \sum_n \ln[1 + T_n(e^p - 1)]. \tag{4.42}$$

The average current follows from $I = \lim_{s\to\infty} s^{-1}\mathbf{e}\langle N(s)\rangle = (\mathbf{e}^2 V_b/h)g$, while the shot-noise power is $P = \lim_{s\to\infty} 2s^{-1}\mathbf{e}^2\langle\langle N(s)^2\rangle\rangle = (2\mathbf{e}^3 V_b/h)\sum_n T_n(1-T_n)$. If all transmission eigenvalues are small, the shot-noise power is $P = 2\mathbf{e}I \equiv P_0$, while in general $P = fP_0$ with the so-called Fano factor $f = \sum_n T_n(1-T_n)/\sum_n T_n \in [0,1]$.

For $N_L = N_R \gg 1$ we can calculate the cumulant-generating function exactly (Blanter *et al.*, 2001),

$$\overline{\ln\langle \exp(pQ(s)/\mathbf{e})\rangle} = s\frac{\mathbf{e}V}{h}\int dT\,\rho(T)\ln[1+T(e^p-1)] = 4sg\frac{\mathbf{e}V}{h}\ln[\frac{1+e^{p/2}}{2}]. \tag{4.43}$$

The Fano factor is then given by $\overline{f} = 1/4$. For $N_L, N_R \gg 1$ not necessarily equal, one finds

$$\overline{f} \approx \frac{N_L N_R}{(N_L+N_R)^2} - (1-2/\beta)\frac{(N_L-N_R)^2}{(N_L+N_R)^3}, \tag{4.44}$$

where the weak-localization correction is seen to vanish if $N_L = N_R$.

As for the decay problem, these transport properties are modified by ballistic transport routes. A wavepacket injected into the opening can leave without any noticeable diffraction until the transport Ehrenfest time $T'_{\mathrm{Ehr}} = \lambda^{-1}\ln N^2/M$ (Silvestrov *et al.*, 2003), which results in transmission eigenvalues T_n close to 0 and 1. In particular, these processes can yield a noticeable suppression of shot noise (Tworzydło *et al.*, 2003).

In the chiral symmetry classes, the statistics of the transmission eigenvalues is most conveniently expressed via $T_n = \sqrt{1-r_n^2}$, where r_n are the eigenvalues of the hermitian matrix $R_z = \tau_z r$ (Macedo-Junior and Macêdo, 2002). We only consider the case $N_L = N_R$ with balanced coupling to both chiral subspaces ($N_A = N_B$), so that $\nu_0 = \operatorname{tr} R_z$ determines the number of zero modes in the closed system. In this case

one encounters $|\nu_0|$ closed transmission channels with $r_n^2 = 1$, while the remaining eigenvalues obey the joined distribution

$$P(\{r_n\}) \propto \prod_{n<m} |r_n - r_m|^\beta \prod_k (1 - r_k^2)^{-1+(|\nu_0|+1)\beta/2}. \tag{4.45}$$

In the symmetry classes with a charge-conjugation symmetry (Dahlhaus *et al.*, 2010),

$$P(\{T_n\}) \propto \prod_{n<m} |T_n - T_m|^{\beta_T} \prod_k T_k^{-1+\beta_T(1+|N_L-N_R|)/2} (1 - T_k)^{\beta_T'/2}, \tag{4.46}$$

where the parameters $\beta_T = 1, 2, 4, 2$, $\beta_T' = -1, -1, 2, 1$ (classes D, DIII, C, CI) are the same as those encountered for the delay times. In the large-N limit, the eigenvalue density becomes again ensemble-independent and approaches (4.37).

Note that the topological quantum number ν_0 only appears in the joint distribution (4.45) for chiral symmetry, but not in the joint distribution (4.46), so that any zero modes due to charge-conjugation symmetry cannot be detected in the transport with ideal leads—the same situation that we encountered for the density of states. This provides an incentive to consider the role of superconductivity and tunnel barriers in such systems, which we here will discuss for the classes D and BDI (Pikulin *et al.*, 2012). Instead of applying the Poisson kernel, we consider the experimentally relevant situation (Mourik *et al.*, 2012) where the tunnel barrier is placed into a normal-conducting region, which is then interfaced with a superconductor.

In the context of such superconducting systems, the dimensionless conductance g relates to the particle (or heat) transport, while the charge transport is modified by the fact that holes carry an opposite charge. If a normal metallic region from the orthogonal symmetry class is attached to a conventional superconductor, the dimensionless conductance for charge transport is given by Eq. (3.8), which applies to systems with no magnetic fields and no spin-orbit scattering. The symmetry classes D arises in the presence of spin-orbit coupling and broken time-reversal symmetry, where only the charge-conjugation symmetry with $\mathcal{C}^2 = 1$ remains. The class BDI emerges from an additional chiral symmetry $\mathcal{X}$ that commutes with $\mathcal{C}$, which then also implies a time-reversal symmetry $\mathcal{T} = \mathcal{X}\mathcal{C}$ with $\mathcal{T}^2 = 1$. In these classes, the dimensionless conductance at the Fermi level can be written as

$$g_{NS} = \operatorname{tr} \Gamma(1 - U^* \sqrt{1-\Gamma} U \sqrt{1-\Gamma})^{-1} \Gamma (1 - U^\dagger \sqrt{1-\Gamma} U^T \sqrt{1-\Gamma})^{-1}, \tag{4.47}$$

where $\Gamma = \operatorname{diag}(T_n)$ while the $N \times N$ dimensional unitary matrix U accounts for the mode-mixing from the spin-orbit scattering. For a large tunnel barrier in the normal region, we can assume that all transmission eigenvalues are identical, $T_n \equiv T$, so that

$$g_{NS} = T^2 \operatorname{tr} \frac{1}{1-(1-T)X} \frac{1}{1-(1-T)X^\dagger} = \sum_n \frac{T^2}{|1-(1-T)x_n|^2} \tag{4.48}$$

is determined by the eigenvalues x_n of $X = U^* U$.

The structure of X implies that all eigenvalues occur in complex conjugated pairs x_n, $x_{\bar{n}} = x_n^*$, with the exception of possible eigenvalues pinned to 1. In class D, where

U is only constrained to be unitary, such an eigenvalue occurs if N is odd; we thus have a topological index $\nu = N \bmod 2$. The paired eigenvalues can be specified by the quantities $\mu_n = (x_n + x_{\bar{n}})/2 = \operatorname{Re} x_n$. Sampling U from the circular unitary ensemble, these quantities then follow the distribution

$$P(\{\mu_n\}) \propto \prod_{n<m} (\mu_n - \mu_m)^2 \prod_k \frac{1+\mu_k}{\sqrt{1-\mu_k^2}} \quad \text{if } \nu = 0, \tag{4.49}$$

$$P(\{\mu_n\}) \propto \prod_{n<m} (\mu_n - \mu_m)^2 \prod_k \sqrt{1-\mu_k^2} \quad \text{if } \nu = 1. \tag{4.50}$$

In class BDI, U is unitary and hermitian, and the number of pinned eigenvalues $|\nu|$ follows from $\nu = \operatorname{tr} U$. Setting $U = V^\dagger \operatorname{diag}(1,1,1,\ldots,-1,-1,-1,\ldots)V$ with V again following the circular unitary ensemble, the paired eigenvalues are then described by the distribution

$$P(\{\mu_n\}) \propto \prod_{n<m} |\mu_n - \mu_m| \prod_k (1-\mu_k)^{(|\nu|-1)/2}. \tag{4.51}$$

The probability distributions (4.49) and (4.51) are both of the form of a Jacobi ensemble (2.15). Including the next-to-leading order in the large-N limit, the density

$$\rho(\mu) = \frac{N}{\pi} \frac{1}{\sqrt{1-\mu^2}} + \frac{1}{2}\delta(\mu-1) - \frac{1}{2}\delta(\mu+1) \tag{4.52}$$

becomes independent of the symmetry class and the topological indices. In leading orders, the ensemble-averaged dimensionless conductance is then given by

$$\overline{g_{NS}} = \frac{NT}{2-T} + \frac{2(1-T)}{(2-T)^2}, \tag{4.53}$$

again irrespective of the symmetry class.

Note that the joint distribution Eq. (4.45) of reflection coefficients in the classes with chiral symmetry can also be interpreted as a Jacobi distribution, while the joint distributions (4.36) and (4.46) can be brought into this form by a suitable shift $T_n = (1-\mu_n)/2$ of the transmission coefficient. We take the appearance of this final class of classical random-matrix ensembles as our cue to wrap up the discussion of fully ergodic elastic scattering. Much more is known, both in terms of technical details as well as in terms of practical applications. This includes the full physical implications of superconductivity, such as Andreev reflection and Josephson currents (Beenakker, 1997; Beenakker, 2015), as well as the interpretation of zero modes in terms of Majorana fermions (Alicea, 2012; Leijnse and Flensberg, 2012; Beenakker, 2013). Another important aspect is the role of physical dimensions, which enters the full classification of topologically protected states (Kitaev, 2009; Teo and Kane, 2010; Ryu *et al.*, 2010; Hasan and Kane, 2010; Qi and Zhang, 2011). In the following chapter 5, we turn to one specific aspect of low-dimensional physics, the phenomenon of Anderson localization which prevents the full exploration of phase space. We also take this as an opportunity for a short detour into interacting systems, for which the related question of thermalization can be addressed by the density matrix.

5
Localization, thermalization and entanglement

To round off these notes we discuss a setting for random-matrix applications which has significance also for interacting systems. This brings us back to the origins of the field, which concerned the energy levels of heavy nuclei (Wigner, 1956; Porter, 1965; Weidenmüller and Mitchell, 2009). There, interactions are sufficient to effectively couple a large number of many-body states, thus resulting in a random Hamiltonian.

Quite generally, statistical methods find broad applications to interacting systems, where the dynamics becomes particularly interesting when one considers low dimensions (Cardy, 1996; Sachdev, 1999). An interesting question is how such systems thermalize (Anderson, 1958; Deutsch, 1991; Srednicki, 1994; Gemmer *et al.*, 2010). Even in absence of interactions, the spread of energy and the propagation of particles can be inhibited by the same wave-interference effects that we so far have taken as the very justification for the application of random-matrix theory. These localization effects, first recognised by Anderson (1958), arise from the sparsity of the underlying matrices, be it due to a reduced coordination number on a lattice, resulting in localization in real space (Kramer and MacKinnon, 1993; Evers and Mirlin, 2008), or due to the presence of interactions that only involve some few-body operators, resulting in localization in Fock space (Basko *et al.*, 2006; Altman and Vosk, 2015; Nandkishore and Huse, 2015). The main question is when this sparsity can be felt, and how.

We first discuss this question briefly for non-interacting systems, where it can be addressed by the impact on the transport properties described in the Section 4.4. We then turn to the many-body setting, where we focus on aspects of thermalization and entanglement.

5.1 Anderson localization

In random-matrix theory, systems with fully chaotic wave scattering are traditionally termed zero-dimensional systems. This is because in practice these systems are often realised by shrinking the size of two or three dimensional systems, as, e.g., in a planar quantum dot or a metallic grain. From a different perspective, such systems could be termed infinite-dimensional, as their main feature is the efficient dynamical coupling of states in the accessible Hilbert space, which is also observed in lattices or graphs with a fixed number of vertices and increasing coordination number. In properly scaled units, we can then assume that all of Hilbert space is instantly explored (ergodic time

$T_{\rm erg} = 0$), so that only one relevant dynamical time scale remains—the dwell time T_D, which characterizes how long a particle will reside within the scattering region.

This approach reaches its limit when the internal transport within the system becomes inefficient. Consider a system made of L random scattering regions placed in series, with contacts carrying $N \gg 1$ channels (Iida *et al.*, 1990). While the dimensionless conductance $g \sim N/2$ of each individual region may be large, the overall conductance $g_L \sim N/(1+L)$ of the composed system shrinks when L is increased. Once $g \lesssim 1$, one finds that the conductance decays exponentially with L, $\ln g_L \sim -2L/\xi$ where $\xi \sim \beta N$ is termed the localization length. The decay arises from a similar exponential decay of the wave functions in the closed system. This phenomenon is known as Anderson localization (Anderson, 1958; Kramer and MacKinnon, 1993; Evers and Mirlin, 2008). Among its many signatures, it results in a significant reduction of the levels repulsion, as energy levels of wave functions localized far apart can approach each other closely. We describe the underlying mechanism in the quasi one-dimensional setting sketched above, which is realised in a long and narrow disordered quantum wire or a disordered wave guide. Anderson localization then occurs at any strength of uncorrelated disorder.

For the detailed statistical description, one composes the system from slices of length L_0 that efficiently scramble all the modes according to a mean free path l, but are small enough so that the effect of each slice can be obtained in perturbation theory (Dorokhov, 1982; Mello *et al.*, 1988; Beenakker, 1997; Nazarov and Blanter, 2009). For $\beta = 2$, one obtains for each step

$$c_n = \frac{l}{L_0}\overline{\delta T_n} = -T_n^2 + 2T_n(1-T_n)\sum_{m\neq n}\frac{T_m}{T_n - T_m}, \quad d_n = \frac{l}{L_0}\overline{(\delta T_n)^2} = 2T_n^2(1-T_n). \tag{5.1}$$

The result can be fed into a Fokker-Planck equation

$$Nl\frac{\partial}{\partial L}P(\{T_n\}) = \sum_n \frac{\partial}{\partial T_n}\left(-c_n + \frac{1}{2}\frac{\partial}{\partial T_n}d_n\right)P(\{T_n\}) \tag{5.2}$$

for the joint distribution of transmission eigenvalues, then known (up to a change of variables) as the Dorokhov-Mello-Pereira-Kumar (DMPK) equation. For this particular symmetry class, the joint distribution can be found exactly by a mapping to a Schrödinger equation describing free fermions (Beenakker and Rejaei, 1993). DMPK equations can also be formulated for the other symmetry classes, where they reveal delocalizing effects near the spectral symmetry points (Brouwer *et al.*, 2002; Brouwer *et al.*, 2005). In the many-channel limit $N \gg 1$, these equations make equivalent predictions to non-linear sigma models (Brouwer and Frahm, 1996; Efetov, 1996), both in the diffusive regime $l \ll L \ll \xi$ as well as in the localised regime $L \gg \xi$. This convergence of models indicates a large degree of universality, which we describe next (Beenakker, 1997).

In the diffusive regime $l \ll L \ll \xi$ of a system with $N \gg 1$ channels, the density of transmission eigenvalues becomes independent of the symmetry class and is given by

$$\rho(T) = \frac{Nl}{2L}\frac{1}{T\sqrt{1-T}} \quad \text{for } T_- < T < 1, \quad T_- \sim 4\exp(-2L/l). \tag{5.3}$$

Including the next-order corrections, the ensemble-averaged dimensionless conductance is $\overline{g} = Nl/L + \frac{1}{3}(1 - 2/\beta)$ and the variance is $\operatorname{var} g = 2/(15\beta)$. Furthermore, $\overline{T(1-T)} = \overline{T}/3$ so that the shot-noise Fano factor is $f = 1/3$.

To capture the universal aspects of Anderson localization for $L \gg \xi$, it is useful to recall that the transfer matrix (3.12) of a composed system follows by multiplication of the transfer matrices of the components, $M = \prod_{l=1}^{L} M_l$. These aspects are therefore linked to products of random matrices (Crisanti *et al.*, 1993; Comtet and Tourigny, 2016). For $L \to \infty$, the eigenvalues $x_n > 1$ of $M^\dagger M$ display an exponential dependence, $\ln x_n \sim 2L/\xi_n$ with Lyapunov exponents ξ_n. The scaled exponents $(\ln x_n)/L$ exhibit diminishing fluctuations, which are captured by a log-normal distribution for x_n.

These general features directly translate to the transmission eigenvalues $T_n = 4/(x_n + 2 + 1/x_n)$. The details follow from the DMPK equation, which recovers the log-normal behaviour of $\ln T_n$ in the localised regime. When ordered by magnitude, the transmission eigenvalues fall into a pattern $1 \gg T_1 \gg T_2 \gg \ldots \gg T_N$, with $\ln T_n \sim -2L(1 + \beta n - \beta)/\xi$ and $\operatorname{var} \ln T \sim 4L/\xi$. The dimensionless conductance is dominated by the largest transmission eigenvalue, and also obeys a log-normal distribution.

These results indicate that the variance $\operatorname{var} \ln g = -2\overline{\ln g}$ in the localized regime is universal. This relation can also be obtained in a diagrammatic approach, where it results from the random-phase approximation (Anderson *et al.*, 1980), and only breaks down when one approaches the band edges, while small corrections are observed near spectral symmetry points in the clean system (Schomerus and Titov, 2003). The strong universality of the log-normal distribution underpins qualitative descriptions based on renormalization arguments, which extend the considerations to higher dimensions (Abrahams *et al.*, 1979). For three dimensions, these arguments predict that localization sets in at a finite disorder strength, which is well supported by numerical investigations (Kramer and MacKinnon, 1993; Evers and Mirlin, 2008). However, an accurate statistical description is still lacking.

5.2 Thermalization and localization in many-body systems

In a low-dimensional many-body system, the localizing properties of disorder can be overcome by interactions. The paradigm is provided by thermal energy fluctuations that can liberate a particle from a trapped state. Such processes are also facilitated by the fact that the many-body level spacing is much smaller than the single-particle level spacing—in fact, with increasing system size the number of available states proliferates exponentially, which can be characterised by an entropy. On the other hand, this proliferation also makes it harder to establish ergodic dynamics (Anderson, 1958; Basko *et al.*, 2006; Altman and Vosk, 2015; Nandkishore and Huse, 2015). For the description of complex interacting systems it is therefore desirable to make contact with quantum statistical mechanics, where the posed questions tie to the concepts of ergodicity, entropy and entanglement (Peres, 2002; Gemmer *et al.*, 2010).

Within the framework of quantum statistical mechanics, thermal equilibrium with a heat bath at temperature T is described by the canonical ensemble with density matrix $\rho = Z^{-1} \exp(-H/T)$, where $Z = \operatorname{tr} \exp(-H/T)$ is the partition function. The additional exchange of particles leads to the grandcanonical ensemble with density matrix $\rho = Z^{-1} \exp((\mu N - H)/T)$, where μ is the chemical potential and N the

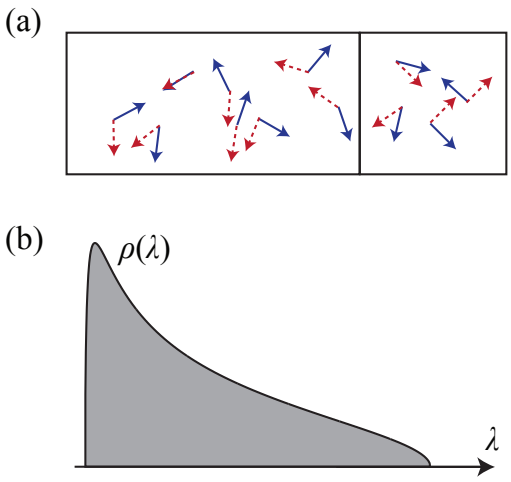

Fig. 5.1 (a) Bipartite entanglement concerns the quantum correlations between a subsystem and its complement. This information is captured in the eigenvalues λ of the reduced density matrix. (b) Up to a small correction accounting for normalisation, the eigenvalues of a random reduced density matrix follow the Marchenko-Pastur law (2.14) for the Wishart-Laguerre ensemble.

fluctuating particle number. In this thermodynamic setting, the associated entropy $\mathcal{S} = -\mathrm{tr}\,\hat{\rho}\ln\hat{\rho}$ is an extensive quantity, which scales linearly with the volume, $\mathcal{S} \propto V_S = O(L^d)$ for a system of size L in d dimensions. This implies that an exponential number $\sim \exp(cV_S)$ of states are populated. Deviations from these predictions occur when one departs from equilibrium. This includes systems in which thermalization is inhibited, with the most notable example found in glasses.

Intriguingly, quantum statistical mechanics also covers the case of closed systems with a fixed energy and particle number, which allows us to focus on the intrinsic quantum-mechanical properties. These systems are described by the microcanonical ensemble, where the density matrix $\rho = M^{-1}\sum_{|E_n-E|<\delta E/2}|\psi_n\rangle\langle\psi_n|$ gives equal weight to $M \gg 1$ eigenstates residing in a classically small energy window δE around a fixed energy E. The expectation that the microcanonical entropy $S = \ln M$ is extensive indicates again that this involves an exponential number of available states.

The applicability of this description is intimately related to the question of thermalization in closed system, which in turn reveals whether the internal dynamics are ergodic (Deutsch, 1991; Srednicki, 1994). These links become apparent when we ask whether the microcanonical ensemble provides a good description of individual time-dependent quantum states. More precisely, we form a generic superposition of the states within the energy window and ask whether the time-averaged expectation values of some well-behaved, preselected observables $\hat{A}_n$ agree with their ensemble averages. As it turns out, a good agreement occurs when the matrix elements of the observables in the basis of participating eigenstates are sufficiently random. The ensuing self-averaging leads to an approximate state-independence of the expectation values—

a phenomenon known as eigenstate thermalization (Srednicki, 1994; Polkovnikov *et al.*, 2011; Nandkishore and Huse, 2015). Deviations from these predictions then serve as an efficient tool to detect inefficient coupling within the system.

In a useful picture, the state of a system becomes mixed because it is entangled with the environment. Given a pure state $|\psi\rangle = \sum_{sb} x_{sb}|s\rangle \otimes |b\rangle \in \mathcal{H}_S \otimes \mathcal{H}_B$, with s labeling basis states of the system and b labeling basis states of the environment, we define the reduced density matrix of the system as $\hat{\rho}_S = \sum_{bss'} x_{sb}x^*_{s'b}|s\rangle\langle s'|$ (Peres, 2002). For an observable $\hat{A} = \hat{A}_S \otimes 1$ that only depends on the state of the system, the expectation value follows from $\mathcal{E}_\psi(A) = \mathrm{tr}\,(\hat{\rho}_S \hat{A}_S)$. The information loss from ignoring the environment can be quantified by the entanglement entropy

$$\mathcal{S}_S = -\mathrm{tr}\,\hat{\rho}_S \ln \hat{\rho}_S = -\sum_k \lambda_k \ln \lambda_k, \tag{5.4}$$

where λ_k are the positive eigenvalues of ρ_S. As indicated, this entropy measures the entanglement between the system and the environment; it vanishes when ρ_S describes a pure state, which requires that $|\psi\rangle = |\psi_S\rangle \otimes |\psi_B\rangle$ is separable.

To apply these concepts to the microcanonical setting of a closed system, we select a subsystem with Hilbert space dimension M and consider the remainder of (still finite) dimension M' as the environment, where for convenience we assume $M' \geq M$. For each normalised eigenstate $|\psi_n\rangle = \sum_{sb} x_{sb}|s\rangle \otimes |b\rangle$, we consider the coefficients x_{sb} as the elements of an $M \times M'$-dimensional matrix x, so that in this basis the reduced density matrix takes the form $\rho_S = xx^\dagger$, while $\rho_B = x^\dagger x$. Both are hermitian, positive semidefinite matrices normalised to $\mathrm{tr}\,\rho_S = \mathrm{tr}\,\rho_B = 1$. The bipartite entanglement entropy follows from Eq. (5.4). As we started out with a pure state for the total system we have $\mathcal{S}_S = \mathcal{S}_B$. Indeed, the non-vanishing eigenvalues of ρ_S and ρ_B are identical, so that we can pair each eigenstate $|\psi_{k,S}\rangle$ of ρ_S with an eigenstate $|\psi_{k,B}\rangle$ of ρ_B. This determines the Schmidt decomposition $|\psi_n\rangle = \sum_k \sqrt{\lambda_k}|\psi_{k,S}\rangle \otimes |\psi_{k,B}\rangle$, which reconstructs the underlying pure eigenstate.

The bipartite entanglement entropy is a useful characteristics if the interactions in the system are local, and plays a central role in a broad range of physical situations, including quantum information (Nielsen and Chuang, 2010) critical phenomena (Calabrese and Cardy, 2009), and quantum gravity (Nishioka *et al.*, 2009). In the ground state of a many-body system with local interactions, the entanglement entropy is found to be small, scaling with the surface area $S_S \propto A_S = O(L^{d-1})$ instead of the volume V_S of the subsystem. This is termed an area law of entanglement. At phase transitions, the entanglement entropy in the ground state increases, and in 1D is often found to display a logarithmic dependence $S_S \sim (c/3)\ln(L)$, where c can be interpreted as the central charge in a conformal field theory (Calabrese and Cardy, 2009).

These considerations can be naturally informed by random-matrix theory, now applied directly to the structure of the eigenstates at a fixed energy. The simplest case arises when we assume that the system displays eigenstate thermalization. This can be modelled by a random reduced density matrix $\rho_S = XX^\dagger/Z$, $Z = \mathrm{tr}\,XX^\dagger$, where X is distributed according to the Gaussian distribution (2.12) (Page, 1993). The density matrix can then be interpreted as a Wishart matrix with posterior normalization (Zyczkowski and Sommers, 2001; Majumdar, 2011). The joint probability density of

the eigenvalues λ_n follows directly by constraining the Wishart-Laguerre ensemble (2.13) to a normalised trace,

$$P(\{\lambda_n\}) \propto \delta\left(1-\sum_k \lambda_k\right) \prod_{n<m} |\lambda_n - \lambda_m|^\beta \prod_k \lambda_k^{\beta(1+M'-M)/2-1}. \tag{5.5}$$

For $1 \ll M \leq M'$, the trace $\sum_k \lambda_k$ is self-averaging. The eigenvalue density then approaches the Marchenko-Pastur law (2.14) with $\overline{\lambda} = 1/M$,

$$\rho(\lambda) = \frac{1}{2\pi\lambda}\sqrt{4MM' - (M+M'-MM'\lambda)^2} \tag{5.6}$$

for $(\sqrt{M'}-\sqrt{M})^2 < MM'\lambda < (\sqrt{M'}+\sqrt{M})^2$. The average entanglement entropy follows as (Page, 1993)

$$\overline{\mathcal{S}_B} = -\int d\lambda\, \rho(\lambda)\lambda \ln\lambda = \ln M - (M/2M'), \tag{5.7}$$

independent of the ensemble. This result signifies near-maximal entanglement. As the Hilbert space dimension of a many-body system grows exponentially with system size, the leading term corresponds to a volume law, $\mathcal{S}_S \propto V_S$, while the subleading term vanishes in the thermodynamic limit $M' \to \infty$. For highly excited states in an ergodic system obeying eigenstate thermalization, we therefore recover the expected thermodynamic behaviour.

Deviations from the eigenstate thermalization conditions should reduce the entanglement entropy. The expectation is that one recovers an area law when the disorder is increased beyond a certain threshold, a phenomenon termed many-body localization (Anderson, 1958; Basko *et al.*, 2006). This transition is indeed confirmed in numerical studies, which also detect a significant reduction of the levels repulsion (Altman and Vosk, 2015; Nandkishore and Huse, 2015). As for the non-interacting case, a complete statistical description of this transition is still missing.

Beyond this setting, many-body systems offer numerous deep applications of random-matrix theory. For instance, the logarithmic scaling in critical one-dimensional systems can be recovered from group integrals over unitary, orthogonal or symplectic matrices equipped with the Haar measure (Keating and Mezzadri, 2005). The ubiquitous appearance of such group integrals in field theories and other setting nicely leads us away from the theory of open quantum systems—see other notes in this issue—so we close here.

6
Conclusions

As these notes illustrate, the applications of random matrices to open quantum systems are very diverse. Indeed, one can reasonably expect that this setting provides natural physical applications for (almost?) any notable random-matrix result. After all, matrices appear naturally in quantum mechanics, while openness liberates us from some of the algebraic constraints otherwise encountered. The relevance comes from the richness of complex dynamics, which helps to justify the approach for generic disorder (Efetov, 1996) or underlying classical chaos (Haake, 2010), and confronts us with a large number of interesting questions about the physical behaviour.

This richness already appeared in the two pure settings covered here—elastic single-particle scattering, and purely interacting systems. The latter topic we only covered briefly, and both effects can of course be combined. This is the subject of much ongoing research—e.g., regarding many-body localization and the topological protection in interacting fermionic systems, to mention just two examples. Furthermore, by combining various effects, links can be established to many other areas that enjoy random-matrix applications, as mentioned at various places in the text. As an example we recall the case of photonic systems with amplification and absorption, for which we can set up effectively non-hermitian descriptions of the wave dynamics. When driven to the laser threshold, these systems provide means to directly probe the poles and residues of the scattering matrix, which gives a physical meaning to the Petermann factor. We can also define new, genuinely non-hermitian symmetries, including the mentioned PT symmetry as well as non-hermitian variants of the chiral and charge-conjugation symmetry, which all provide interesting topological effects. Such systems also display nonlinear phenomena, for which entirely new descriptions need to be developed.

It is of course important to consider where the predictive power of random-matrix descriptions may end. Take the design of small quantum devices. While their dedicated functionality is beyond the scope, random-matrix theory can still help to determine how well they may work—as is illustrated by our discussion of entanglement. Our system may also be insufficiently ergodic. For instance, localization effects in low dimensions lead to the search for new ensembles, a search that has not been completed. More subtle effects can arise from ballistic dynamics. These are the short-time signatures of classically deterministic motion captured by the fractal Weyl law, and dynamical constraints as encountered in a classically mixed (partially regular and chaotic) phase space. Given some suitable questions, random-matrix theory can often still be adapted to such situations, and otherwise serves as a useful benchmark to quantify the system-specific behaviour. In general, deviations from random-matrix predictions can indicate exciting novel physics, leading to an endeavour that is nowhere near to end.

Appendix A
Eigenvalue densities of matrices with large dimensions

In the limit of large matrix dimensions M, eigenvalue distributions can be obtained very efficiently by applications of potential theory, which are based on the analogy of eigenvalues with fictitious particles in a Coulomb gas (Dyson, 1962*b*; Dyson, 1972; Beenakker, 1997; Forrester, 2010). In the case of the Gaussian ensembles, the leading order can also be obtained from self-consistent equations for the Green function (or resolvent) G (Pastur and Shcherbina, 2011). The latter approach links neatly to the theory of free probability (Janik *et al.*, 1997; Janik *et al.*, 1999), as we exploit in the following.

A.1 Gaussian hermitian ensembles

For the Gaussian ensembles of hermitian matrices H, we expand the Green function $G(E) = (E - H + i\varepsilon)^{-1}$ in a geometric series

$$G = E^{-1} \sum_{n=0}^{\infty} (HE^{-1})^n \tag{A.1}$$

and average using Wick's theorem, but only retaining non-crossing contractions,

$$\overline{G} = E^{-1} + E^{-1} \overline{\dot{H} E^{-1} \sum_{n=0}^{\infty} (HE^{-1})^n \dot{H} E^{-1} \sum_{n=0}^{\infty} (HE^{-1})^n}, \tag{A.2}$$

where the dot denotes terms that remain to be contracted. Denoting the variance $\overline{|H_{lm}|^2} = \sigma^2$ this gives in leading order $\overline{G} = E^{-1} + E^{-1}\sigma^2 (\operatorname{tr} \overline{G}) \overline{G}$. In terms of the trace $g = \operatorname{tr} \overline{G}$, this leads to Pastur's equation

$$E = \sigma^2 \, g + M/g. \tag{A.3}$$

The solution $g = (1/2\sigma^2)\sqrt{E^2 - 4M\sigma^2}$ determines the density of states via

$$\rho(E) = -\lim_{\varepsilon \to 0^+} \frac{1}{\pi} \operatorname{Im} g(E + i\varepsilon) = \frac{2M}{\pi E_0^2} \sqrt{E_0^2 - E^2} \tag{A.4}$$

for $|E| < E_0$, where we identified $\sigma^2 = M\Delta^2/\pi^2 = E_0^2/4M$. This is the semicircle law (2.3). In the language of free probability, Eq. (A.3) leads to the notion of a Blue function $B_r(z) = \sigma_r^2 g + M/g$, where for later reference we equipped the variance with an index.

A.2 Wishart-Laguerre ensembles

For the Wishart-Laguerre ensembles, we analogously write

$$G(\lambda) = (\lambda - X^\dagger X)^{-1} = \lambda^{-1} \sum_{n=0}^{\infty} (X^\dagger X \lambda^{-1})^n \tag{A.5}$$

and express the non-crossing contractions as

$$\overline{G} = \lambda^{-1} + \dot{X}^\dagger \overline{(\lambda - XX^\dagger)^{-1}} \dot{X} \overline{G} = \lambda^{-1} + \sigma^2 \overline{\mathrm{tr}(\lambda - XX^\dagger)^{-1}} \overline{G} \tag{A.6}$$

with $\overline{|X_{lm}|^2} = \sigma^2$. As $XX^\dagger$ differs from $X^\dagger X$ by $M' - M$ vanishing eigenvalues, we obtain

$$g = \lambda^{-1} M + \sigma^2 (\lambda^{-1}(M' - M) + g) g, \tag{A.7}$$

where again $g = \mathrm{tr}\, \overline{G}$. The solution

$$g = \frac{1}{2\sigma^2} - \frac{M' - M}{2\lambda} \pm \frac{1}{2\lambda\sigma^2} \sqrt{\lambda^2 - 2\lambda\sigma^2(M + M') + \sigma^4 (M - M')^2} \tag{A.8}$$

gives the Marchenko-Pastur law (2.14) via $\rho(\lambda) = -\frac{1}{\pi} \mathrm{Im}\, g$.

Note that in the chiral ensembles with Hamiltonian (2.4), the eigenvalues E_n^2 can be obtained from a Wishart matrix $AA^\dagger$; the joint distributions (2.13) and (2.5) are thus related by a change of variables $\lambda_n \propto E_n^2$, and so are the densities (2.14) and (2.7).

A.3 Jacobi ensembles

For the Jacobi ensembles, we base the considerations on the matrix $(X^\dagger X)^{-1} Y^\dagger Y$, whose eigenvalues λ_n determine the eigenvalues of the MANOVA matrix $(X^\dagger X + Y^\dagger Y)^{-1} X^\dagger X$ by $T_n = 1/(1 + \lambda_n)$. Consider the Green function

$$G = \begin{pmatrix} \lambda & Y \\ Y^\dagger & XX^\dagger - \lambda' \end{pmatrix} = \begin{pmatrix} G_{11} & G_{12} \\ G_{21} & G_{22} \end{pmatrix}, \quad g = \begin{pmatrix} \mathrm{tr}\, G_{11} & \mathrm{tr}\, G_{12} \\ \mathrm{tr}\, G_{21} & \mathrm{tr}\, G_{22} \end{pmatrix}. \tag{A.9}$$

This has matrix elements

$$G_{11} = [\lambda - Y(X^\dagger X - \lambda')^{-1} Y^\dagger]^{-1}, \quad G_{22} = (X^\dagger X - \lambda' - Y^\dagger Y/\lambda)^{-1}, \tag{A.10}$$

with traces

$$g_{11} = (M_y - M)/\lambda + g_0, \quad \mathrm{tr}\, X G_{22} X^\dagger = \lambda' g_{22} + \lambda g_0, \tag{A.11}$$

where

$$g_0 = \mathrm{tr}[\lambda - (X^\dagger X - \lambda')^{-1} Y^\dagger Y]^{-1}. \tag{A.12}$$

The eigenvalue density can then be obtained from $\rho(\lambda) = -\pi^{-1} \mathrm{Im}\, \overline{g_0}|_{\lambda'=0}$.

The non-crossing contractions give the relation

$$\overline{G} = \begin{pmatrix} 1/\lambda & 0 \\ 0 & -1/\lambda' \end{pmatrix} + \sigma^2 \begin{pmatrix} \mathrm{tr}\,\overline{G_{22}}/\lambda & 0 \\ 0 & -\mathrm{tr}\,\overline{G_{11}}/\lambda' \end{pmatrix} \overline{G} + (\sigma^2/\lambda') \begin{pmatrix} 0 & 0 \\ 0 & M_x - \mathrm{tr}\,\overline{X G_{22} X^\dagger} \end{pmatrix} \overline{G}, \tag{A.13}$$

while on average $\overline{G_{12}} = \overline{G_{21}} = 0$. For $\lambda' \to 0$, we therefore have

$$\overline{g_{11}} = M_y/\lambda + \sigma^2 \overline{g_{11}}\,\overline{g_{22}}/\lambda, \quad 0 = M + \sigma^2[(1+\lambda)\overline{g_{11}} + M - M_x - M_y]\overline{g_{22}}, \tag{A.14}$$

which determines

$$\overline{g_0} = \frac{(M+M_x)\lambda + M - M_y - \sqrt{[(M-M_x)\lambda + M - M_y]^2 - 4M_x M_y \lambda}}{2\pi\lambda(1+\lambda)}. \tag{A.15}$$

Denoting $c_x = M_x/M$, $c_y = M_y/M$, the eigenvalue density is thus given by

$$\rho(\lambda) = \frac{M(c_x - 1)\sqrt{(\lambda - \lambda_-)(\lambda_+ - \lambda)}}{2\pi\lambda(1+\lambda)}, \tag{A.16}$$

where

$$\lambda_\pm = \left(\frac{\sqrt{c_x c_y} \pm \sqrt{c_x + c_y - 1}}{c_x - 1} \right)^2 = \left(\frac{c_y - 1}{\sqrt{c_x c_y} \mp \sqrt{c_x + c_y - 1}} \right)^2 \tag{A.17}$$

determines the range where the density is finite. In terms of the variables T_n, the density is then given by Eq. (2.16).

A.4 Ginibre ensembles

As an example of non-hermitian matrix ensembles we consider the complex Ginibre ensemble, defined by (2.12) with $\beta = 2$. The Green function has now to be extended to the block form (Janik *et al.*, 1999)

$$G(z,z^*) = \begin{pmatrix} z - X & i\lambda \\ i\lambda & z^* - X^\dagger \end{pmatrix}^{-1} = \begin{pmatrix} G_{11} & G_{12} \\ G_{21} & G_{22} \end{pmatrix}, \quad g(z,z^*) = \lim_{\lambda \to 0^+} \begin{pmatrix} \mathrm{tr}\,G_{11} & \mathrm{tr}\,G_{12} \\ \mathrm{tr}\,G_{21} & \mathrm{tr}\,G_{22} \end{pmatrix}, \tag{A.18}$$

which delivers the density of complex eigenvalues z_m via

$$\frac{1}{\pi}\frac{\partial g_{11}}{\partial z^*} = \rho(z) = \sum_m \delta(z - z_m), \tag{A.19}$$

while the Petermann factors K_m are encoded in

$$-\frac{1}{\pi} g_{12} g_{21} = O(z) = \sum_m K_m \delta(z - z_m). \tag{A.20}$$

We denote again $\overline{|X_{lm}|^2} = \sigma^2$ and employ the expansion

$$G = \mathfrak{Z}^{-1} \sum_{n=0}^{\infty} (\mathfrak{x}\mathfrak{Z}^{-1})^n, \quad \mathfrak{Z} = \begin{pmatrix} z & i\lambda \\ i\lambda & z^* \end{pmatrix}, \quad \mathfrak{x} = \begin{pmatrix} X & 0 \\ 0 & X^\dagger \end{pmatrix}, \tag{A.21}$$

followed by the non-crossing approximation

$$\overline{G} = \mathfrak{Z}^{-1} + \mathfrak{Z}^{-1} \overline{\dot{\mathfrak{x}}\mathfrak{Z}^{-1} \sum_{n=0}^{\infty} (\mathfrak{x}\mathfrak{Z}^{-1})^n \dot{\mathfrak{x}}\mathfrak{Z}^{-1}} \, \overline{\sum_{n=0}^{\infty} (\mathfrak{x}\mathfrak{Z}^{-1})^n} \tag{A.22}$$

$$= \mathfrak{Z}^{-1} + \mathfrak{Z}^{-1}\sigma^2 \begin{pmatrix} 0 & \overline{g_{12}} \\ \overline{g_{21}} & 0 \end{pmatrix} \overline{G}, \tag{A.23}$$

where the dot denotes elements to be Wick-contracted. The trace gives

$$\mathfrak{Z} = M/\overline{g} + \frac{\sigma^2}{2}(\overline{g} + \tilde{g}), \quad \tilde{g} = \begin{pmatrix} 1 & 0 \\ 0 & -1 \end{pmatrix} \overline{g} \begin{pmatrix} -1 & 0 \\ 0 & 1 \end{pmatrix}. \tag{A.24}$$

This agrees with the rules from free probability, according to which the Blue functions of the real and imaginary parts are $B_r(A) = \sigma_r^2 A + M/A$, $B_i(A) = \sigma_i^2 \tilde{A} + M/A$, while the composition law reads $\mathfrak{Z} = B_r(g) + B_i(g) - M/g$; here $\sigma_r^2 = \sigma_i^2 = \sigma^2/2$.

Let us set $\sigma^2 = 1/M$. For $|z| < 1$ the solution is then given by

$$\overline{g} = M \begin{pmatrix} z^* & \sqrt{|z^2| - 1} \\ \sqrt{|z^2| - 1} & z \end{pmatrix}. \tag{A.25}$$

From this we recover Ginibre's circular law $\rho(z) = \frac{M}{\pi}\Theta(1 - |z|)$, while $O(z) = M^2(1 - |z|^2)/\pi$. According to Eq. (A.20), the ratio $O(z)/\rho(z) = M(1 - |z|^2) \sim \overline{K_m}|_{z_m = z}$ gives the average Petermann factor within the support of the spectrum.

References

Abrahams, E., Anderson, P. W., Licciardello, D. C., and Ramakrishnan, T. V. (1979). Scaling theory of localization: Absence of quantum diffusion in two dimensions. *Phys. Rev. Lett.*, **42**, 673–676.

Akemann, G. (2017). Random matrix theory and quantum chromodynamics. arXiv:1603.06011.

Akemann, G., Baik, J., and Di Francesco, P. (ed.) (2011). *The Oxford Handbook of Random Matrix Theory*, Oxford, New York. Oxford University Press.

Akhmerov, A. R., Dahlhaus, J. P., Hassler, F., Wimmer, M., and Beenakker, C. W. J. (2011). Quantized conductance at the Majorana phase transition in a disordered superconducting wire. *Phys. Rev. Lett.*, **106**, 057001.

Aleiner, I. L. and Larkin, A. I. (1996). Divergence of classical trajectories and weak localization. *Phys. Rev. B*, **54**, 14423–14444.

Alicea, J. (2012). New directions in the pursuit of Majorana fermions in solid state systems. *Rep. Prog. Phys.*, **75**, 076501.

Altland, A. and Zirnbauer, M. R. (1997). Nonstandard symmetry classes in mesoscopic normal-superconducting hybrid structures. *Phys. Rev. B*, **55**, 1142–1161.

Altman, E. and Vosk, R. (2015). Universal dynamics and renormalization in many-body-localized systems. *Annu. Rev. Condens. Matter Phys.*, **6**, 383–409.

Anderson, P. W. (1958). Absence of diffusion in certain random lattices. *Phys. Rev.*, **109**, 1492–1505.

Anderson, P. W., Thouless, D. J., Abrahams, E., and Fisher, D. S. (1980). New method for a scaling theory of localization. *Phys. Rev. B*, **22**, 3519–3526.

Bäcker, A. (2003). Numerical aspects of eigenvalue and eigenfunction computations for chaotic quantum systems. In *The Mathematical Aspects of Quantum Maps* (ed. M. D. Esposito and S. Graffi), Volume 618, Lecture Notes in Physics, Berlin, p. 91. Springer.

Baranger, H. U. and Mello, P. A. (1994). Mesoscopic transport through chaotic cavities: A random s-matrix theory approach. *Phys. Rev. Lett.*, **73**, 142–145.

Basko, D. M., Aleiner, I. L., and Altshuler, B. L. (2006). Metal-insulator transition in a weakly interacting many-electron system with localized single-particle states. *Ann. Phys. (N. Y.)*, **321**, 1126–1205.

Beenakker, C. W. J. (1992). Quantum transport in semiconductor-superconductor microjunctions. *Phys. Rev. B*, **46**, 12841–12844.

Beenakker, C. W. J. (1997). Random-matrix theory of quantum transport. *Rev. Mod. Phys.*, **69**, 731–808.

Beenakker, C. W. J. (1998). Thermal radiation and amplified spontaneous emission from a random medium. *Phys. Rev. Lett.*, **81**, 1829–1832.

Beenakker, C. W. J. (2005). Andreev billiards. *Lecture Notes in Physics*, **667**, 131–174. arXiv:cond-mat/0406018.

Beenakker, C. W. J. (2013). Search for Majorana fermions in superconductors. *Annu. Rev. Condens. Matter Phys.*, **4**, 113–136.

Beenakker, C. W. J. (2015). Random-matrix theory of Majorana fermions and topological superconductors. *Rev. Mod. Phys.*, **87**, 1037–1066.

Beenakker, C. W. J., Edge, J. M., Dahlhaus, J. P., Pikulin, D. I., Mi, Shuo, and Wimmer, M. (2013). Wigner-poisson statistics of topological transitions in a josephson junction. *Phys. Rev. Lett.*, **111**, 037001.

Beenakker, C. W. J. and Rejaei, B. (1993). Nonlogarithmic repulsion of transmission eigenvalues in a disordered wire. *Phys. Rev. Lett.*, **71**, 3689–3692.

Bender, C. M. (2007). Making sense of non-Hermitian Hamiltonians. *Rep. Prog. Phys.*, **70**, 947.

Béri, B. (2009). Random scattering matrices for Andreev quantum dots with nonideal leads. *Phys. Rev. B*, **79**, 214506.

Berman, G. P. and Zaslavsky, G. M. (1978). Condition of stochasticity in quantum nonlinear systems. *Physica A*, **91**, 450–460.

Berry, M. V. (2004). Physics of Nonhermitian Degeneracies. *Czech. J. Phys.*, **54**, 1039–1047.

Birchall, C. and Schomerus, H. (2012). Random-matrix theory of amplifying and absorbing resonators with $\mathcal{PT}$ or $\mathcal{PTT}'$ symmetry. *J. Phys. A.*, **45**, 444006.

Birman, M. S. and Krein, M. G. (1962). On the theory of wave operators and scattering operators. *Sov. Math. Dokl.*, **3**, 740–744.

Blanter, Ya. M. and Büttiker, M. (2000). Shot noise in mesoscopic conductors. *Phys. Rep.*, **336**, 1–166.

Blanter, Ya. M., Schomerus, H., and Beenakker, C. W. J. (2001). Effect of dephasing on charge-counting statistics in chaotic cavities. *Physica E*, **11**, 1–7.

Blümel, R. and Smilansky, U. (1990). Random-matrix description of chaotic scattering: Semiclassical approach. *Phys. Rev. Lett.*, **64**, 241–244.

Breuer, H.-P. and Petruccione, F. (2002). *The Theory of Open Quantum Systems*. Oxford University Press, Oxford.

Brouwer, P. W. (1995). Generalized circular ensemble of scattering matrices for a chaotic cavity with nonideal leads. *Phys. Rev. B*, **51**, 16878–16884.

Brouwer, P. W. (1998). Scattering approach to parametric pumping. *Phys. Rev. B*, **58**, R10135–R10138.

Brouwer, P. W. and Frahm, K. (1996). Quantum transport in disordered wires: Equivalence of the one-dimensional σ model and the Dorokhov-Mello-Pereyra-Kumar equation. *Phys. Rev. B*, **53**, 1490–1501.

Brouwer, P. W., Frahm, K. M., and Beenakker, C. W. J. (1997). Quantum mechanical time-delay matrix in chaotic scattering. *Phys. Rev. Lett.*, **78**, 4737–4740.

Brouwer, P. W., Furusaki, A., Mudry, C., and Ryu, S. (2005). Disorder-induced critical phenomena–new universality classes in Anderson localization. *eprint arXiv:cond-mat/0511622*.

Brouwer, P. W., Racine, E., Furusaki, A., Hatsugai, Y., Morita, Y., and Mudry, C. (2002). Zero modes in the random hopping model. *Phys. Rev. B*, **66**, 014204.

Büttiker, M. (1990). Scattering theory of thermal and excess noise in open conductors. *Phys. Rev. Lett.*, **65**, 2901–2904.

Büttiker, M., Thomas, H., and Prêtre, A. (1994). Current partition in multiprobe conductors in the presence of slowly oscillating external potentials. *Z. Phys. B*, **94**, 133–137.

Calabrese, P. and Cardy, J. (2009). Entanglement entropy and conformal field theory. *J. Phys. A.*, **42**, 504005.

Cao, H. and Wiersig, J. (2015). Dielectric microcavities: Model systems for wave chaos and non-hermitian physics. *Rev. Mod. Phys.*, **87**, 61–111.

Cardy, J. (1996). *Scaling and Renormalization in Statistical Physics.* Cambridge Lecture Notes in Physics. Cambridge University Press, Cambridge, New York.

Carmichael, H. (2009). *An Open Systems Approach to Quantum Optics.* Lecture Notes in Physics Monographs. Springer, Berlin, Heidelberg.

Caselle, M. and Magnea, U. (2004). Random matrix theory and symmetric spaces. *Phys. Rep.*, **394**, 41–156.

Chalker, J. T. and Mehlig, B. (1998). Eigenvector statistics in non-hermitian random matrix ensembles. *Phys. Rev. Lett.*, **81**, 3367–3370.

Comtet, A. and Tourigny, Y. (2016). Impurity models and products of random matrices. arXiv:1601.01822.

Crisanti, A., Paladin, G., and Vulpiani, A. (1993). *Products of Random Matrices.* Volume 104, Springer Series in Solid-State Sciences. Springer, Berlin, Heidelberg.

Dahlhaus, J. P., Béri, B., and Beenakker, C. W. J. (2010). Random-matrix theory of thermal conduction in superconducting quantum dots. *Phys. Rev. B*, **82**, 014536.

Datta, S. (1997). *Electronic Transport in Mesoscopic Systems.* Cambridge University Press, Cambridge, New York.

de Carvalho, C. A. A. and Nussenzveig, H. M. (2002). Time delay. *Phys. Rep.*, **364**, 83–174.

Deutsch, J. M. (1991). Quantum statistical mechanics in a closed system. *Phys. Rev. A*, **43**, 2046–2049.

Dorokhov, O. N. (1982). Transmission coefficient and the localization length of an electron in n bound disordered chains. *JETP Lett.*, **36**, 318–321.

Doron, E. and Smilansky, U. (1992). Semiclassical quantization of chaotic billiards: a scattering theory approach. *Nonlinearity*, **5**, 1055.

Dyson, F. J. (1962*a*). Statistical theory of the energy levels of complex systems. I. *J. Math. Phys.*, **3**, 140–156.

Dyson, F. J. (1962*b*). Statistical theory of the energy levels of complex systems. II. *J. Math. Phys.*, **3**, 157–165.

Dyson, F. J. (1962*c*). The threefold way. algebraic structure of symmetry groups and ensembles in quantum mechanics. *J. Math. Phys.*, **3**, 1199–1215.

Dyson, F. J. (1970). Correlations between eigenvalues of a random matrix. *Comm. Math. Phys.*, **19**, 235–250.

Dyson, F. J. (1972). A class of matrix ensembles. *J. Math. Phys.*, **13**, 90–97.

Efetov, K. (1996). *Supersymmetry in disorder and chaos.* Cambridge University Press, Cambridge, New York.

Evers, F. and Mirlin, A. D. (2008). Anderson transitions. *Rev. Mod. Phys.*, **80**,

1355–1417.

Forrester, P. J. (2010). *Log-Gases and Random Matrices*. Princeton University Press, Princeton.

Forrester, P. J. and Nagao, T. (2007). Eigenvalue Statistics of the Real Ginibre Ensemble. *Phys. Rev. Lett.*, **99**, 050603.

Fu, L. and Kane, C. L. (2008). Superconducting proximity effect and Majorana fermions at the surface of a topological insulator. *Phys. Rev. Lett.*, **100**, 096407.

Fulga, I. C., Hassler, F., Akhmerov, A. R., and Beenakker, C. W. J. (2011). Scattering formula for the topological quantum number of a disordered multimode wire. *Phys. Rev. B*, **83**, 155429.

Fyodorov, Y. V. and Khoruzhenko, B. A. (1999). Systematic analytical approach to correlation functions of resonances in quantum chaotic scattering. *Phys. Rev. Lett.*, **83**, 65–68.

Fyodorov, Y. and Savin, D. (2011). Resonance scattering of waves in chaotic systems. See Akemann, Baik and Di Francesco (2011).

Fyodorov, Y. V. and Savin, D. V. (2012). Statistics of resonance width shifts as a signature of eigenfunction nonorthogonality. *Phys. Rev. Lett.*, **108**, 184101.

Fyodorov, Y. V. and Sommers, H.-J. (1996). Statistics of S-matrix poles in few-channel chaotic scattering: Crossover from isolated to overlapping resonances. *JETP Lett.*, **63**, 1026–1030.

Fyodorov, Y. V. and Sommers, H.-J. (1997). Statistics of resonance poles, phase shifts and time delays in quantum chaotic scattering: Random matrix approach for systems with broken time-reversal invariance. *J. Math. Phys.*, **38**, 1918–1981.

Fyodorov, Y. V. and Sommers, H.-J. (2000). Spectra of random contractions and scattering theory for discrete-time systems. *JETP Lett.*, **72**, 422–426.

Fyodorov, Y. V. and Sommers, H.-J. (2003). Random matrices close to Hermitian or unitary: overview of methods and results. *J. Phys. A.*, **36**, 3303–3347.

Gasparian, V., Christen, T., and Büttiker, M. (1996). Partial densities of states, scattering matrices, and green's functions. *Phys. Rev. A*, **54**, 4022–4031.

Gemmer, J., Michel, M., and Mahler, G. (2010). *Quantum Thermodynamics*. Volume 784, Lecture Notes in Physics. Springer, Berlin, Heidelberg.

Ginibre, J. (1965). Statistical Ensembles of Complex, Quaternion, and Real Matrices. *J. Math. Phys.*, **6**, 440.

Girko, V. L. (1986). Elliptic Law. *Theor. Prob. Appl.*, **30**, 677–690.

Guhr, T., Müller-Groeling, A., and Weidenmüller, H. A. (1998). Random-matrix theories in quantum physics: common concepts. *Phys. Rep.*, **299**, 189–425.

Haake, F. (2010). *Quantum Signatures of Chaos*. Volume 54, Springer Series in Synergetics. Springer, Berlin, Heidelberg.

Haake, F., Izrailev, F., Lehmann, N., Saher, D., and Sommers, H.-J. (1992). Statistics of complex levels of random matrices for decaying systems. *Z. Phys. B*, **88**, 359–370.

Hasan, M. Z. and Kane, C. L. (2010). *Colloquium*: Topological insulators. *Rev. Mod. Phys.*, **82**, 3045–3067.

Heiss, W. D. (2012). The physics of exceptional points. *J. Phys. A: Math. Theor.*, **45**, 444016.

Iida, S., Weidenmüller, H. A., and Zuk, J. A. (1990). Statistical scattering theory,

the supersymmetry method and universal conductance fluctuations. *Ann. Phys. (N. Y.)*, **200**, 219–270.

Jalabert, R. A., Pichard, J.-L., and Beenakker, C. W. J. (1994). Universal quantum signatures of chaos in ballistic transport. *EPL (Europhysics Letters)*, **27**, 255.

Janik, R. A., Nörenberg, W., Nowak, M. A., Papp, G., and Zahed, I. (1999). Correlations of eigenvectors for non-Hermitian random-matrix models. *Phys. Rev. E*, **60**, 2699–2705.

Janik, R. A., Nowak, M. A., Papp, G., Wambach, J., and Zahed, I. (1997). Non-Hermitian random matrix models: Free random variable approach. *Phys. Rev. E*, **55**, 4100–4106.

Keating, J. P. and Mezzadri, F. (2005). Entanglement in quantum spin chains, symmetry classes of random matrices, and conformal field theory. *Phys. Rev. Lett.*, **94**, 050501.

Keating, J. P., Novaes, M., Prado, S. D., and Sieber, M. (2006). Semiclassical structure of chaotic resonance eigenfunctions. *Phys. Rev. Lett.*, **97**, 150406.

Khoruzhenko, B. and Sommers, H.-J. (2011). Non-hermitian ensembles. See Akemann, Baik and Di Francesco (2011).

Kitaev, A. (2009). Periodic table for topological insulators and superconductors. *AIP Conference Proceedings*, **1134**, 22–30.

Kitagawa, T., Berg, E., Rudner, M., and Demler, E. (2010). Topological characterization of periodically driven quantum systems. *Phys. Rev. B*, **82**, 235114.

Kramer, B. and MacKinnon, A. (1993). Localization: theory and experiment. *Rep. Prog. Phys.*, **56**, 1469.

Lehmann, N., Saher, D., Sokolov, V. V., and Sommers, H.-J. (1995). Chaotic scattering: the supersymmetry method for large number of channels. *Nucl. Phys. A*, **582**, 223–256.

Lehmann, N. and Sommers, H.-J. (1991). Eigenvalue statistics of random real matrices. *Phys. Rev. Lett.*, **67**, 941–944.

Leijnse, M. and Flensberg, K. (2012). Introduction to topological superconductivity and Majorana fermions. *Semicond. Sci. Technol.*, **27**, 124003.

Levitov, L. S. and Lesovik, G. B. (1993). Charge distribution in quantum shot noise. *JETP Lett.*, **58**, 230.

Lieb, E. H. (1989). Two theorems on the Hubbard model. *Phys. Rev. Lett.*, **62**, 1201–1204.

Livsic, M. S. (1973). *Operators, Oscillations, Waves*. American Mathematical Society, Providence, RI.

Lu, L., Joannopoulos, J. D., and Soljačić, M. (2014). Topological photonics. *Nat. Photon.*, **8**, 821–829.

Lu, W. T., Sridhar, S., and Zworski, M. (2003). Fractal Weyl laws for chaotic open systems. *Phys. Rev. Lett.*, **91**, 154101.

Macedo-Junior, A. F. and Macêdo, A. M. S. (2002). Universal transport properties of quantum dots with chiral symmetry. *Phys. Rev. B*, **66**, 041307.

Magnea, U. (2008). Random matrices beyond the Cartan classification. *J. Phys. A*, **41**, 045203.

Mahaux, C. and Weidenmüller, H. A. (1969). *Shell-model approach to nuclear reactions*. North-Holland, Amsterdam, London.

Majumdar, S. N. (2011). Extreme eigenvalues of wishart matrices and entangled bipartite system. See Akemann, Baik and Di Francesco (2011).

Makris, K. G., El-Ganainy, R., Christodoulides, D. N., and Musslimani, Z. H. (2008). Beam dynamics in $\mathcal{PT}$ symmetric optical lattices. *Phys. Rev. Lett.*, **100**, 103904.

Malzard, S., Poli, C., and Schomerus, H. (2015). Topologically protected defect states in open photonic systems with non-hermitian charge-conjugation and parity-time symmetry. *Phys. Rev. Lett.*, **115**, 200402.

Marčenko, V. A. and Pastur, L. A. (1967). Distribution of eigenvalues for some sets of random matrices. *Math. USSR-Sb.*, **1**, 457.

Marciani, M., Brouwer, P. W., and Beenakker, C. W. J. (2014). Time-delay matrix, midgap spectral peak, and thermopower of an Andreev billiard. *Phys. Rev. B*, **90**, 045403.

Marciani, M., Schomerus, H., and Beenakker, C. W. J. (2016). Effect of a tunnel barrier on the scattering from a Majorana bound state in an Andreev billiard. *Physica E*, **77**, 54–64.

Mehta, M. L. (2004). *Random Matrices*. Pure and Applied Mathematics. Elsevier Science, Amsterdam.

Mello, P. A., Pereyra, P., and Kumar, N. (1988). Macroscopic approach to multichannel disordered conductors. *Ann. Phys. (N. Y.)*, **181**, 290–317.

Messiah, A. (2014). *Quantum Mechanics*. Dover Books on Physics. Dover Publications, Mineola, N.Y.

Moiseyev, N. (2011). *Non-Hermitian Quantum Mechanics*. Cambridge University Press, Cambridge, New York.

Mourik, V., Zuo, K., Frolov, S. M., Plissard, S. R., Bakkers, E. P. a. M., and Kouwenhoven, L. P. (2012). Signatures of Majorana fermions in hybrid superconductor-semiconductor nanowire devices. *Science*, **336**, 1003–1007.

Nandkishore, R. and Huse, D. A. (2015). Many-body localization and thermalization in quantum statistical mechanics. *Annu. Rev. Condens. Matter Phys.*, **6**, 15–38.

Nayak, C., Simon, S. H., Stern, A., Freedman, M., and Das Sarma, S. (2008). Non-abelian anyons and topological quantum computation. *Rev. Mod. Phys.*, **80**, 1083–1159.

Nazarov, Y. V. and Blanter, Ya. M. (2009). *Quantum Transport: Introduction to Nanoscience*. Cambridge University Press, Cambridge, New York.

Newton, R. G. (2002). *Scattering theory of waves and particles*. Dover Publications, Mineola, N.Y.

Nielsen, M. A. and Chuang, I. L. (2010). *Quantum Computation and Quantum Information*. Cambridge University Press, Cambridge, New York.

Nishioka, T., Ryu, S., and Takayanagi, T. (2009). Holographic entanglement entropy: an overview. *J. Phys. A.*, **42**, 504008.

Nonnenmacher, S. and Zworski, M. (2005). Fractal Weyl laws in discrete models of chaotic scattering. *J. Phys. A.*, **38**, 10683–10682.

Page, D. N. (1993). Average entropy of a subsystem. *Phys. Rev. Lett.*, **71**, 1291–1294.

Pastur, L. A. and Shcherbina, M. (2011). *Eigenvalue Distribution of Large Random*

Matrices. Mathematical surveys and monographs. American Mathematical Society, Providence.

Peres, A. (2002). *Quantum Theory: Concepts and Methods*. Springer, Dordrecht.

Petermann, K. (1979). Calculated spontaneous emission factor for double-heterostructure injection lasers with gain-induced waveguiding. *IEEE J. Quantum Electron.*, **15**, 566–570.

Pikulin, D. I., Dahlhaus, J. P., Wimmer, M., Schomerus, H., and Beenakker, C. W. J. (2012). A zero-voltage conductance peak from weak antilocalization in a Majorana nanowire. *New J. Phys.*, **14**, 125011.

Pikulin, D. I. and Nazarov, Yu. V. (2012). Topological properties of superconducting junctions. *JETP Lett.*, **94**, 693–697.

Pikulin, D. I. and Nazarov, Y. V. (2013). Two types of topological transitions in finite Majorana wires. *Phys. Rev. B*, **87**, 235421.

Poli, C., Bellec, M., Kuhl, U., Mortessagne, F., and Schomerus, H. (2015). Selective enhancement of topologically induced interface states in a dielectric resonator chain. *Nature Communications*, **6**, 6710.

Polkovnikov, A., Sengupta, K., Silva, A., and Vengalattore, M. (2011). *Colloquium*: Nonequilibrium dynamics of closed interacting quantum systems. *Rev. Mod. Phys.*, **83**, 863–883.

Porter, C. E. (1965). *Statistical Theory of Spectra: Fluctuations*. Academic Press, New York.

Qi, X.-L. and Zhang, S.-C. (2011). Topological insulators and superconductors. *Rev. Mod. Phys.*, **83**, 1057–1110.

Rotter, I. (2009). A non-hermitian hamilton operator and the physics of open quantum systems. *J. Phys. A.*, **42**, 153001.

Rüter, C. E., Makris, K. G., El-Ganainy, R., Christodoulides, D. N., Segev, M., and Kip, D. (2010). Observation of parity-time symmetry in optics. *Nat. Phys.*, **6**, 192–195.

Ryu, S., Schnyder, A. P., Furusaki, A., and Ludwig, A. W. W. (2010). Topological insulators and superconductors: tenfold way and dimensional hierarchy. *New J. Phys.*, **12**, 065010.

Sachdev, S. (1999). *Quantum phase transitions*. Cambridge University Press, Cambridge, New York.

San-Jose, P., Cayao, J., Prada, E., and Aguado, R. (2016). Majorana bound states from exceptional points in non-topological superconductors. *Sci. Rep.*, **6**, 21427.

Savin, D. V. and Sokolov, V. V. (2013). Quantum versus classical decay laws in open chaotic systems. *Phys. Rev. E*, **56**, R4911–R4913.

Schomerus, H. (2009). Excess quantum noise due to mode nonorthogonality in dielectric microresonators. *Phys. Rev. A*, **79**, 061801.

Schomerus, H. (2010). Quantum noise and self-sustained radiation of PT-symmetric systems. *Phys. Rev. Lett.*, **104**, 233601.

Schomerus, H. (2013*a*). From scattering theory to complex wave dynamics in non-Hermitian PT-symmetric resonators. *Phil. Trans. R. Soc. A*, **371**, 20120194.

Schomerus, H. (2013*b*). Topologically protected midgap states in complex photonic lattices. *Opt. Lett.*, **38**, 1912.

Schomerus, H., Frahm, K. M., Patra, M., and Beenakker, C. W. J. (2000). Quantum limit of the laser line width in chaotic cavities and statistics of residues of scattering matrix poles. *Physica A*, **278**, 469–496.

Schomerus, H. and Halpern, N. Y. (2013). Parity Anomaly and Landau-Level Lasing in Strained Photonic Honeycomb Lattices. *Phys. Rev. Lett.*, **110**, 013903.

Schomerus, H. and Jacquod, P. (2005). Quantum-to-classical correspondence in open chaotic systems. *J. Phys. A.*, **38**, 10663.

Schomerus, H., Marciani, M., and Beenakker, C. W. J. (2015). Effect of chiral symmetry on chaotic scattering from Majorana zero modes. *Phys. Rev. Lett.*, **114**, 166803.

Schomerus, H. and Titov, M. (2003). Band-center anomaly of the conductance distribution in one-dimensional anderson localization. *Phys. Rev. B*, **67**, 100201.

Schomerus, H. and Tworzydło, J. (2004). Quantum-to-classical crossover of quasibound states in open quantum systems. *Phys. Rev. Lett.*, **93**, 154102.

Schomerus, H., Wiersig, J., and Main, J. (2009). Lifetime statistics in chaotic dielectric microresonators. *Phys. Rev. A*, **79**, 053806.

Silvestrov, P. G., Goorden, M. C., and Beenakker, C. W. J. (2003). Noiseless scattering states in a chaotic cavity. *Phys. Rev. B*, **67**, 241301.

Smith, F. T. (1960). Lifetime matrix in collision theory. *Phys. Rev.*, **118**, 349–356.

Sommers, H.-J., Fyodorov, Y. V., and Titov, M. (1999). S-matrix poles for chaotic quantum systems as eigenvalues of complex symmetric random matrices: from isolated to overlapping resonances. *J. Phys. A: Math. Gen.*, **32**, L77.

Srednicki, M. (1994). Chaos and quantum thermalization. *Phys. Rev. E*, **50**, 888–901.

Stöckmann, H.-J. (2006). *Quantum Chaos: An Introduction.* Cambridge University Press, Cambridge, New York.

Sutherland, B. (1986). Localization of electronic wave functions due to local topology. *Phys. Rev. B*, **34**, 5208–5211.

Teo, J. C. Y. and Kane, C. L. (2010). Topological defects and gapless modes in insulators and superconductors. *Phys. Rev. B*, **82**, 115120.

Texier, C. (2016). Wigner time delay and related concepts: Application to transport in coherent conductors. *Physica E*, **82**, 16–33.

Tworzydło, J., Tajic, A., Schomerus, H., and Beenakker, C. W. J. (2003). Dynamical model for the quantum-to-classical crossover of shot noise. *Phys. Rev. B*, **68**, 115313.

Verbaarschot, J. J. M. (1994). The spectrum of the QCD Dirac operator and chiral random matrix theory: The threefold way. *Phys. Rev. Lett.*, **72**, 2531–2533.

Verbaarschot, J. J. M., Weidenmüller, H. A., and Zirnbauer, M. R. (1985). Grassmann integration in stochastic quantum physics: The case of compound-nucleus scattering. *Phys. Rep.*, **129**, 367–438.

Verbaarschot, J. J. M. and Wettig, T. (2000). Random matrix theory and chiral symmetry in QCD. *Annu. Rev. Nucl. Part. Sci.*, **50**, 343–410.

Weich, T., Barkhofen, S., Kuhl, U., Poli, C., and Schomerus, H. (2014). Formation and interaction of resonance chains in the open three-disk system. *New J. Phys.*, **16**, 033029.

Weidenmüller, H. A. and Mitchell, G. E. (2009). Random matrices and chaos in nuclear physics: Nuclear structure. *Rev. Mod. Phys.*, **81**, 539–589.

Weiss, U. (2008). *Quantum Dissipative Systems* (3rd edn). World Scientific, Singapore.

Wiersig, J. (2014). Enhancing the sensitivity of frequency and energy splitting detection by using exceptional points: Application to microcavity sensors for single-particle detection. *Phys. Rev. Lett.*, **112**, 203901.

Wigner, E. P. (1955). Lower limit for the energy derivative of the scattering phase shift. *Phys. Rev.*, **98**, 145–147.

Wigner, E. P. (1956). Proceedings of the conference on neutron physics by time-of-flight. *ORNL-Report*, **2309**, 59–70.

Wigner, E. P. (1958). On the distribution of the roots of certain symmetric matrices. *Ann. Math.*, **67**, 325–327.

Wishart, J. (1928). The generalised product moment distribution in samples from a normal multivariate population. *Biometrika*, **20A**, 32–52.

Yoo, G., Sim, H.-S., and Schomerus, H. (2011). Quantum noise and mode nonorthogonality in non-Hermitian $\mathcal{PT}$-symmetric optical resonators. *Phys. Rev. A*, **84**(6), 063833.

Zirnbauer, M. (2011). Symmetry classes. See Akemann, Baik and Di Francesco (2011).

Zirnbauer, M. R. (1996). Riemannian symmetric superspaces and their origin in random-matrix theory. *J. Math. Phys.*, **37**, 4986–5018.

Zyczkowski, K. and Sommers, H.-J. (2000). Truncations of random unitary matrices. *J. Phys. A.*, **33**, 2045.

Zyczkowski, K. and Sommers, H.-J. (2001). Induced measures in the space of mixed quantum states. *J. Phys. A.*, **34**, 7111.